

A WELL BALANCED FINITE VOLUME SCHEME FOR GENERAL RELATIVITY

ELENA GABURRO*, MANUEL J. CASTRO†, AND MICHAEL DUMBSER‡

Abstract. In this work we present a novel second order accurate well balanced (WB) finite volume (FV) scheme for the solution of the general relativistic magnetohydrodynamics (GRMHD) equations and the first order CCZ4 formulation (FO-CCZ4) of the Einstein field equations of general relativity, as well as the fully coupled FO-CCZ4 + GRMHD system. These systems of *first order hyperbolic* PDEs allow to study the dynamics of the *matter* and the dynamics of the *space-time* according to the theory of general *relativity*.

The new well balanced finite volume scheme presented here exploits the knowledge of an equilibrium solution of interest when integrating the conservative fluxes, the nonconservative products and the algebraic source terms, and also when performing the piecewise linear data reconstruction. This results in a rather simple modification of the underlying second order FV scheme, which, however, being able to cancel numerical errors committed with respect to the equilibrium component of the numerical solution, substantially improves the accuracy and long-time stability of the numerical scheme when simulating small perturbations of stationary equilibria. In particular, the need for well balanced techniques appears to be more and more crucial as the applications increase their complexity. We close the paper with a series of numerical tests of increasing difficulty, where we study the evolution of small perturbations of accretion problems and stable TOV neutron stars. Our results show that the well balancing significantly improves the long-time stability of the finite volume scheme compared to a standard one.

Key words. first order hyperbolic systems, finite volume schemes (FV), well balanced schemes (WB), general relativistic magnetohydrodynamics (GRMHD), first order conformal and covariant reformulation of the Einstein field equations (FO-CCZ4), Michel accretion disk, TOV neutron star.

AMS subject classifications. 35L40, 65M08, 83C05, 83C10, 85-08, 85-10, 85A30.

1. Introduction. The main goal of this work is to improve the long-term stability and accuracy of finite volume schemes in the context of numerical general relativity. The models that we consider here are the general relativistic Euler and magnetohydrodynamics (GRMHD) equations [17, 6, 11, 48, 49, 57] and the so-called first order CCZ4 formulation (FO-CCZ4) of the Einstein field equations [3, 55, 54]. The governing PDE systems in general relativity are extremely challenging since they contain not only very complex equations with many unknowns, but some systems are also subject to involution constraints that affect hyperbolicity and thus well-posedness of the initial value problem. Moreover, the applications of interest in this field, such as the evolution of accretion disks, neutron stars and black holes, are characterized by a disparity of the involved space and time scales: indeed, we need to observe the *long time evolution* of phenomena developing over *astronomical distances*, such as gravitational waves, but whose behavior is strongly affected by physical perturbations developed at smaller scales like a binary neutron star system. Furthermore, it is particularly challenging to simulate small perturbations of stationary equilibria when the perturbations are of the order of the numerical discretization error. Hence, the main objective of this paper consists in improving long-time stability and accuracy of numerical methods for the simulation of astrophysical phenomena occurring close to

*INRIA, Univ. Bordeaux, CNRS, Bordeaux INP, IMB, UMR 5251, 200 Avenue de la Vieille Tour, 33405 Talence cedex, France (elena.gaburro@inria.fr).

†Department of Mathematical Analysis, Statistics and Applied Mathematics, University of Málaga, Campus de Teatinos, 29071 Málaga, Spain (mjcastro@uma.es).

‡Department of Civil, Environmental and Mechanical Engineering, University of Trento, Via Mesiano 77, 38123 Trento, Italy (michael.dumbser@unitn.it).

44 stationary equilibrium solutions of the GRMHD and FO-CCZ4 equations. This will
 45 be achieved thanks to the introduction of modern well balancing (WB) techniques (see
 46 for example [23, 74, 38, 39, 62, 40] and the references therein) inside the finite volume
 47 scheme that allow to preserve given equilibria of the governing PDE system *exactly*
 48 at the discrete level, thus avoiding that small physical perturbations are masked by
 49 numerical discretization errors. To the best of our knowledge, this is the very first
 50 time that an exactly well balanced finite volume scheme is proposed for the GRMHD
 51 and FO-CCZ4 equations of numerical general relativity, for a given set of relevant
 52 stationary solutions.

53 A brief literature review on the state of the art of numerical general relativity as
 54 well as on existing well balanced techniques for computational fluid dynamics in the
 55 context of free surface shallow water flows and the Euler equations of gasdynamics
 56 with Newtonian gravity is given below.

57 The GRMHD model combines the fluid description of matter with a simplified
 58 theory for electromagnetic fields in the absence of free charge carriers. It was studied
 59 for the first time in [100, 9, 87] and [8], without and with electromagnetic fields. Sub-
 60 stantial progress in the field has been made by the group of Ibañez and co-workers,
 61 who introduced the now universally adopted *Valencia formulation* of general relativistic
 62 hydrodynamics and magnetohydrodynamics, see e.g. [17, 11, 58, 75] and references
 63 therein. There, the GRHD and GRMHD systems have been cast into conservation
 64 law form, which allowed to apply classical Godunov-type finite volume schemes for
 65 hyperbolic equations. Subsequently, many different solvers have been developed, see
 66 for example [16, 52, 10, 49, 65, 7, 71, 31, 83, 51, 84, 99, 82]. Other studies incorporate
 67 radiation transfer, like the one proposed by [91], or include the full Maxwell theory
 68 in a resistive relativistic MHD formulation [79, 56, 51, 32, 33, 5]. Here we follow
 69 the approach of [57], where the gravitational field in fixed background space-time
 70 (Cowling approximation) are treated via the use of *nonconservative products* instead
 71 of the usually employed algebraic source terms, since gravity terms can be expressed
 72 as functions of the spatial derivatives of the lapse, the shift vector and the spatial
 73 metric tensor, i.e. some of the conserved variables.

74 Besides the evolution of the matter, the numerical integration of the Einstein field
 75 equations for the time evolution of the metric is another challenging problem. The
 76 covariant nature of the equations allows the choice of arbitrary moving curvilinear
 77 coordinates (gauge freedom), and hence first a suitable set of space-time coordinates
 78 must be chosen. The first step in this direction was achieved with the 3+1 (space +
 79 time) ADM formulation of [12], see also [13, 20], which allowed to rewrite the Einstein
 80 field equations as an initial boundary value problem, but the proposed PDE system
 81 was not hyperbolic. A mixed elliptic-hyperbolic formalism, know as fully constrained
 82 formulation (FCF) was then proposed in [28] and its mathematical structure, well-
 83 posedness and uniqueness were further analyzed in [46, 45]. Then, among the first
 84 hyperbolic formulations was the BSSNOK (Baumgarte-Shapiro-Shibata-Nakamura-
 85 Oohara-Kojima) formulation [89, 19, 77]. Subsequently, different alternative formu-
 86 lations were proposed, like the Z4 formulation [25, 26, 2], the Z4c system [24] and
 87 the CCZ4 in [3, 4]. For an exhaustive overview of different models used in numerical
 88 general relativity, see [1]. Most of the previous formulations led to first order sys-
 89 tems in time, but with first and second order derivatives in space, and were therefore
 90 not directly accessible for standard Godunov-type methods for first order hyperbolic
 91 systems. Instead, the systems were typically integrated with high order central finite
 92 difference schemes. The problem of hyperbolicity of different second order in space

formulations of general relativity was discussed in [68]. The PDE system used in this paper is based on the first order CCZ4 formulation (FO-CCZ4) that has been derived in [55] and for which strong hyperbolicity has been demonstrated for a particular choice of gauges. In [54], the curl-free condition of certain evolution variables of the FO-CCZ4 system was taken into account via a novel hyperbolic generalized Lagrangian multiplier (GLM) *curl-cleaning* technique.

Numerical simulations of GRMHD and FO-CCZ4 at the aid of high order DG schemes with *a posteriori* subcell finite volume limiter have been presented in [57, 55, 54], showing the appropriateness of the chosen governing PDE systems and the numerical methods employed for their solution. However, the obtained results also clearly indicate that with standard schemes for hyperbolic PDE one can reach only rather short simulation times (w.r.t astrophysical timescales) and rather fine meshes (w.r.t astrophysical spatial scales) are required, even for the simulation of stationary equilibrium solutions of the governing PDE systems. Thus, there is a necessity to endow existing methods with the ability of preserving additional physical properties of the underlying PDE system in such a way that spurious numerical modes can be eliminated, numerical dissipation reduced and small-scale structures can manifest inside large-scale macroscopic models. In Newtonian computational fluid dynamics, such improved properties of a numerical scheme can be achieved at the aid of well balancing (WB), which allows to preserve certain stationary equilibrium solutions of the governing PDE system *exactly* at the discrete level. In the pioneering work of Bermúdez and Vázquez in 1994 [23] the authors have proposed an exactly well balanced Roe solver for lake at rest solutions of the shallow water equations. Further important results in this field have been achieved in [30, 15, 85, 38, 66, 74, 81, 92, 39]. More recent works are, for example, [64, 61, 42, 21, 40, 14]. Since it is impossible to mention all the relevant references here, we refer to the recent review paper [40], which besides an interesting treatment of discontinuous equilibria contains a rather complete review of the wide literature on well balanced schemes. Finally, we would like to underline that the development of WB and structure preserving schemes for astrophysical applications is a topic of growing interest, although the existing works so far only employ much simpler Newtonian PDE systems, see for example [29, 69, 70, 41, 88, 50, 22, 62, 72, 67, 93] and the references therein, where well balanced schemes for the Euler equations of gasdynamics with Newtonian gravity were proposed.

The rest of the paper is organized as follows. In Section 2 we introduce the governing PDE systems that are solved in this paper; in Section 3 we present our new well balanced second order finite volume scheme for numerical general relativity that allows to preserve smooth equilibria exactly at the discrete level. The increased stability and resolution gained with the use of the new scheme are shown via a series of numerical tests of increasing difficulty presented in Section 4. We close the paper with some remarks and an outlook to future works in Section 5.

2. Governing PDE systems. All governing PDE systems for numerical general relativity used throughout this paper can be written as first order hyperbolic partial differential equations of the following general form:

$$(2.1) \quad \mathbf{Q}_t + \nabla \cdot \mathbf{F}(\mathbf{Q}) + \mathbf{B}(\mathbf{Q}) \cdot \nabla \mathbf{Q} = \mathbf{S}(\mathbf{Q}), \quad \mathbf{x} = (x_1, x_2, x_3) \in \Omega \subset \mathbb{R}^3,$$

where $\mathbf{x} = (x_1, x_2, x_3) = (x, y, z)$ is the spatial position vector, t represents the time, Ω is the computational domain, $\mathbf{Q} = (q_1, q_2, \dots, q_m)^T$ is the state vector defined in the space of the admissible states $\Omega_{\mathbf{Q}} \subset \mathbb{R}^m$, $\mathbf{F}(\mathbf{Q}) = (\mathbf{f}(\mathbf{Q}), \mathbf{g}(\mathbf{Q}), \mathbf{h}(\mathbf{Q}))$ is the non linear flux tensor, $\mathbf{B}(\mathbf{Q}) = (\mathbf{B}_1(\mathbf{Q}), \mathbf{B}_2(\mathbf{Q}), \mathbf{B}_3(\mathbf{Q}))$ is a matrix collecting the nonconserva-

141 tive terms, and $\mathbf{S}(\mathbf{Q})$ represents a nonlinear algebraic source term. The form (2.1) is
 142 said to be *hyperbolic* if for all directions $\mathbf{n} \neq \mathbf{0}$ the matrix $\mathbf{A}_n = (\partial\mathbf{F}/\partial\mathbf{Q} + \mathbf{B}(\mathbf{Q})) \cdot \mathbf{n}$
 143 has m real eigenvalues and a full set of m linearly independent eigenvectors.

144 In this work we will consider problems that, due to their spherical symmetry, can
 145 be written as *one-dimensional* hyperbolic PDE systems of the type

$$146 \quad (2.2) \quad \mathbf{Q}_t + \mathbf{f}_x(\mathbf{Q}) + \mathbf{B}_1(\mathbf{Q}) \cdot \mathbf{Q}_x = \mathbf{S}(\mathbf{Q}) - \mathbf{S}_b(\mathbf{Q}, \mathbf{Q}_y, \mathbf{Q}_z),$$

147 where in \mathbf{S}_b we collect eventual non-zero terms depending on derivatives of the state
 148 variables with respect to the y and z coordinates. Throughout this paper we employ
 149 the Einstein summation convention, which implies summation over two repeated in-
 150 dices and we use Greek letters for four-dimensional indices running from 0 to 3 and
 151 Latin letters for three-dimensional indices running from 1 to 3. We work in a ge-
 152 ometrized set of units, in which the speed of light and the gravitational constant are
 153 set to unity, i.e. $c = G = 1$.

154 The complete set of governing equations of the fully coupled FO-CCZ4 + GRMHD
 155 system reads as follows (see [55, 54] and [57]):

$$156 \quad (2.3a) \quad \partial_t \tilde{\gamma}_{ij} = \beta^k 2D_{kij} + \tilde{\gamma}_{ki} B_j^k + \tilde{\gamma}_{kj} B_i^k - \frac{2}{3} \tilde{\gamma}_{ij} B_k^k - 2\alpha \left(\tilde{A}_{ij} - \frac{1}{3} \tilde{\gamma}_{ij} \text{tr} \tilde{A} \right),$$

$$157 \quad (2.3b) \quad \partial_t \ln \alpha = \beta^k A_k - \alpha g(\alpha)(K - K_0 - 2\Theta c), \quad \partial_t K_0 = 0,$$

$$158 \quad (2.3c) \quad \partial_t \beta^i = s \beta^k B_k^i + s f b^i,$$

$$159 \quad (2.3d) \quad \partial_t \ln \phi = \beta^k P_k + \frac{1}{3} (\alpha K - B_k^k),$$

160

$$161 \quad \partial_t \tilde{A}_{ij} - \beta^k \partial_k \tilde{A}_{ij} + \phi^2 \left[\nabla_i \nabla_j \alpha - \alpha (R_{ij} + \nabla_i Z_j + \nabla_j Z_i - 8\pi S_{ij}) \right]$$

$$162 \quad - \frac{1}{3} \tilde{\gamma}_{ij} \left[\nabla^k \nabla_k \alpha - \alpha (R + 2\nabla_k Z^k - 8\pi S) \right]$$

$$163 \quad (2.4a) \quad = \tilde{A}_{ki} B_j^k + \tilde{A}_{kj} B_i^k - \frac{2}{3} \tilde{A}_{ij} B_k^k + \alpha \tilde{A}_{ij} (K - 2\Theta c) - 2\alpha \tilde{A}_{il} \tilde{\gamma}^{lm} \tilde{A}_{mj},$$

164

$$165 \quad \partial_t K - \beta^k \partial_k K + \nabla^i \nabla_i \alpha - \alpha (R + 2\nabla_i Z^i)$$

$$166 \quad (2.4b) \quad = \alpha K (K - 2\Theta c) - 3\alpha \kappa_1 (1 + \kappa_2) \Theta + 4\pi \alpha (S - 3\tau),$$

167

$$168 \quad \partial_t \Theta - \beta^k \partial_k \Theta - \frac{1}{2} \alpha e^2 (R + 2\nabla_i Z^i)$$

$$169 \quad (2.4c) \quad = \alpha e^2 \left(\frac{1}{3} K^2 - \frac{1}{2} \tilde{A}_{ij} \tilde{A}^{ij} - 8\pi \tau \right) - \alpha \Theta K c - Z^i \alpha A_i - \alpha \kappa_1 (2 + \kappa_2) \Theta,$$

170

$$171 \quad \partial_t \hat{\Gamma}^i - \beta^k \partial_k \hat{\Gamma}^i + \frac{4}{3} \alpha \tilde{\gamma}^{ij} \partial_j K - \tilde{\gamma}^{kl} \partial_{(k} B_{l)}^i - \tilde{\gamma}^{ik} \left(\frac{1}{3} \partial_{(k} B_{l)}^l + s 2\alpha \tilde{\gamma}^{nm} \partial_k \tilde{A}_{nm} + 2\alpha \partial_k \Theta \right)$$

$$172 \quad = \frac{2}{3} \tilde{\Gamma}^i B_k^k - \tilde{\Gamma}^k B_k^i + 2\alpha \left(\tilde{\Gamma}_{jk}^i \tilde{A}^{jk} - 3\tilde{A}^{ij} P_j \right) - 2\alpha \tilde{\gamma}^{ki} \left(\Theta A_k + \frac{2}{3} K Z_k \right) - 2\alpha \tilde{A}^{ij} A_j$$

$$173 \quad - 4s \alpha \tilde{\gamma}^{ik} D_k^{nm} \tilde{A}_{nm} + 2\kappa_3 \left(\frac{2}{3} \tilde{\gamma}^{ij} Z_j B_k^k - \tilde{\gamma}^{jk} Z_j B_k^i \right) - 2\alpha \kappa_1 \tilde{\gamma}^{ij} Z_j - 16\pi \alpha \tilde{\gamma}^{ij} S_j,$$

$$174 \quad (2.4d)$$

$$175 \quad (2.4e) \quad \partial_t b^i - s \beta^k \partial_k b^i = s \left(\partial_t \hat{\Gamma}^i - \beta^k \partial_k \hat{\Gamma}^i - \eta b^i \right).$$

176 The use of the logarithms in the evolution equations for the lapse and the conformal factor is for convenience, in order to always guarantee *positivity* of α and ϕ also
 177 at the *discrete level*. In order to obtain a strongly hyperbolic first-order reduction,
 178 the following evolution system for the auxiliary variables $A_k := \partial_k \alpha / \alpha$, $B_k^i := \partial_k \beta^i$,
 179 $D_{kij} := \frac{1}{2} \partial_k \tilde{\gamma}_{ij}$ and $P_k := \partial_k \phi / \phi$ is added, accounting also for the stationary involu-
 180 tions of the governing PDE system:
 181

$$182 \quad \partial_t A_k - \beta^l \partial_l A_k + \alpha g(\alpha) (\partial_k K - \partial_k K_0 - 2c \partial_k \Theta) + s \alpha g(\alpha) \tilde{\gamma}^{nm} \partial_k \tilde{A}_{nm}$$

$$183 \quad (2.5a) \quad = +2s \alpha g(\alpha) D_k^{nm} \tilde{A}_{nm} - \alpha A_k (K - K_0 - 2\Theta c) h(\alpha) + B_k^l A_l,$$

$$184 \quad \partial_t B_k^i - s \beta^l \partial_l B_k^i - s (f \partial_k b^i - \alpha^2 \mu \tilde{\gamma}^{ij} (\partial_k P_j - \partial_j P_k))$$

$$185 \quad (2.5b) \quad - s (\alpha^2 \mu \tilde{\gamma}^{ij} \tilde{\gamma}^{nl} (\partial_k D_{ljn} - \partial_l D_{kjn})) = s B_k^l B_l^i,$$

$$186 \quad \partial_t D_{kij} - \beta^l \partial_l D_{kij} + s \left(-\frac{1}{2} \tilde{\gamma}_{mi} \partial_{(k} B_{j)}^m - \frac{1}{2} \tilde{\gamma}_{mj} \partial_{(k} B_{i)}^m + \frac{1}{3} \tilde{\gamma}_{ij} \partial_{(k} B_{m)}^m \right)$$

$$187 \quad + \alpha \partial_k \tilde{A}_{ij} - \alpha \frac{1}{3} \tilde{\gamma}_{ij} \tilde{\gamma}^{nm} \partial_k \tilde{A}_{nm} = B_k^l D_{lij} + B_j^l D_{kli} + B_i^l D_{klj} - \frac{2}{3} B_l^l D_{kij}$$

$$188 \quad (2.5c) \quad - \alpha \frac{2}{3} \tilde{\gamma}_{ij} D_k^{nm} \tilde{A}_{nm} - \alpha A_k \left(\tilde{A}_{ij} - \frac{1}{3} \tilde{\gamma}_{ij} \text{tr} \tilde{A} \right),$$

$$189 \quad \partial_t P_k - \beta^l \partial_l P_k - \frac{1}{3} \alpha \partial_k K + \frac{1}{3} \partial_{(k} B_{i)}^i - s \frac{1}{3} \alpha \tilde{\gamma}^{nm} \partial_k \tilde{A}_{nm}$$

$$190 \quad (2.5d) \quad = \frac{1}{3} \alpha A_k K + B_k^l P_l - s \frac{2}{3} \alpha D_k^{nm} \tilde{A}_{nm}.$$

191 The matter and magnetic field evolution equations, which are *fully coupled* with the
 192 above FO-CCZ4 system read:

$$193 \quad (2.6) \quad \partial_t (\sqrt{\gamma} D) + \partial_i \left(\gamma^{\frac{1}{2}} (\alpha v^i D - \beta^i D) \right) = 0,$$

$$194 \quad \partial_t (\sqrt{\gamma} S_j) + \partial_i \left(\gamma^{\frac{1}{2}} (\alpha T_j^i - \beta^i S_j) \right)$$

$$195 \quad (2.7) \quad = \gamma^{\frac{1}{2}} (\alpha T^{ik} C_{jik} + S_i B_j^i - \alpha \tau A_j),$$

$$196 \quad \partial_t (\sqrt{\gamma} \tau) + \partial_i \left(\gamma^{\frac{1}{2}} (\alpha (S^i - v^i D) - \beta^i \tau) \right)$$

$$197 \quad (2.8) \quad = \gamma^{\frac{1}{2}} (\alpha K_{ij} T^{ij} - \alpha S^j A_j),$$

$$198 \quad (2.9) \quad \partial_t (\sqrt{\gamma} B^j) + \partial_i \left(\gamma^{\frac{1}{2}} ((\alpha v^i - \beta^i) B^j - (\alpha v^j - \beta^j) B^i + \varphi \delta^{ij}) \right) = 0,$$

$$199 \quad (2.10) \quad \partial_t (\sqrt{\gamma} \varphi) + \partial_i \left(\gamma^{\frac{1}{2}} (\alpha c_h^2 B^i - \beta^i \varphi) \right) = 0,$$

200 with the abbreviation $C_{kij} = \frac{1}{\phi^2} (D_{kij} - P_k \tilde{\gamma}_{ij})$ and where T^{ij} denotes the spatial
 201 stress-energy tensor

$$202 \quad T^{ij} := \rho h W^2 v^i v^j - E^i E^j - B^i B^j + \left[p + \frac{1}{2} (E^2 + B^2) \right] \gamma^{ij}$$

$$203 \quad (2.11) \quad = S^i v^j + p_{\text{tot}} \gamma^{ij} - \frac{B^i B^j}{W^2} - (B_k v^k) v^i B^j,$$

204 with the enthalpy $\rho h = \rho + \frac{\gamma}{\gamma-1} p$, the total pressure defined as

$$205 \quad (2.12) \quad p_{\text{tot}} = p + p_{\text{mag}} = p + \frac{1}{2} [B^2 / W^2 + (B \cdot v)^2].$$

206 The governing PDE system (2.3a)–(2.5d) contains the terms defined below:

$$\begin{aligned}
207 \quad & \text{tr} \tilde{A} = \tilde{\gamma}^{ij} \tilde{A}_{ij}, \quad \text{and} \quad \tilde{\gamma} = \det(\tilde{\gamma}_{ij}), \\
208 \quad & \partial_k \tilde{\gamma}^{ij} = -2\tilde{\gamma}^{in} \tilde{\gamma}^{mj} D_{knm} := -2D_k^{ij}, \\
209 \quad & \tilde{\Gamma}_{ij}^k = \tilde{\gamma}^{kl} (D_{ijl} + D_{jil} - D_{lij}), \\
210 \quad & \partial_k \tilde{\Gamma}_{ij}^m = -2D_k^{ml} (D_{ijl} + D_{jil} - D_{lij}) + \tilde{\gamma}^{ml} (\partial_{(k} D_{i)jl} + \partial_{(k} D_{j)il} - \partial_{(k} D_{l)ij}), \\
211 \quad & \Gamma_{ij}^k = \tilde{\gamma}^{kl} (D_{ijl} + D_{jil} - D_{lij}) - \tilde{\gamma}^{kl} (\tilde{\gamma}_{jl} P_i + \tilde{\gamma}_{il} P_j - \tilde{\gamma}_{ij} P_l) \\
212 \quad & = \tilde{\Gamma}_{ij}^k - \tilde{\gamma}^{kl} (\tilde{\gamma}_{jl} P_i + \tilde{\gamma}_{il} P_j - \tilde{\gamma}_{ij} P_l), \\
213 \quad & \partial_k \Gamma_{ij}^m = -2D_k^{ml} (D_{ijl} + D_{jil} - D_{lij}) + 2D_k^{ml} (\tilde{\gamma}_{jl} P_i + \tilde{\gamma}_{il} P_j - \tilde{\gamma}_{ij} P_l) \\
214 \quad & \quad - 2\tilde{\gamma}^{ml} (D_{kjl} P_i + D_{kil} P_j - D_{kij} P_l) \\
215 \quad & \quad + \tilde{\gamma}^{ml} (\partial_{(k} D_{i)jl} + \partial_{(k} D_{j)il} - \partial_{(k} D_{l)ij}) \\
216 \quad & \quad - \tilde{\gamma}^{ml} (\tilde{\gamma}_{jl} \partial_{(k} P_i) + \tilde{\gamma}_{il} \partial_{(k} P_j) - \tilde{\gamma}_{ij} \partial_{(k} P_l)), \\
217 \quad & R_{ikj}^m = \partial_k \Gamma_{ij}^m - \partial_j \Gamma_{ik}^m + \Gamma_{ij}^l \Gamma_{lk}^m - \Gamma_{ik}^l \Gamma_{lj}^m, \quad R_{ij} = R_{imj}^m, \\
218 \quad & \nabla_i \nabla_j \alpha = \alpha A_i A_j - \alpha \Gamma_{ij}^k A_k + \alpha \partial_{(i} A_{j)}, \quad \nabla^i \nabla_i \alpha = \phi^2 \tilde{\gamma}^{ij} (\nabla_i \nabla_j \alpha), \\
219 \quad & \tilde{\Gamma}^i = \tilde{\gamma}^{jl} \tilde{\Gamma}_{jl}^i, \\
220 \quad & \partial_k \tilde{\Gamma}^i = -2D_k^{jl} \tilde{\Gamma}_{jl}^i + \tilde{\gamma}^{jl} \partial_k \tilde{\Gamma}_{jl}^i, \\
221 \quad & Z_i = \frac{1}{2} \tilde{\gamma}_{ij} (\hat{\Gamma}^j - \tilde{\Gamma}^j), \quad Z^i = \frac{1}{2} \phi^2 (\hat{\Gamma}^i - \tilde{\Gamma}^i), \\
222 \quad & \nabla_i Z_j = D_{ijl} (\hat{\Gamma}^l - \tilde{\Gamma}^l) + \frac{1}{2} \tilde{\gamma}_{jl} (\partial_i \hat{\Gamma}^l - \partial_i \tilde{\Gamma}^l) - \Gamma_{ij}^l Z_l, \\
223 \quad & R + 2\nabla_k Z^k = \phi^2 \tilde{\gamma}^{ij} (R_{ij} + \nabla_i Z_j + \nabla_j Z_i), \\
224 \quad & h(\alpha) = \left(g(\alpha) + \alpha \frac{\partial g(\alpha)}{\partial \alpha} \right).
\end{aligned}$$

225 The function $g(\alpha)$ in the PDE for the lapse α controls the slicing condition, where
226 $g(\alpha) = 1$ leads to harmonic slicing and $g(\alpha) = 2/\alpha$ leads to the so-called 1+log slicing
227 condition, see [27]. As already mentioned above, the auxiliary quantities A_k , P_k , B_k^i
228 and D_{kij} are defined as (scaled) spatial gradients of the primary variables α , ϕ , β^i
229 and $\tilde{\gamma}_{ij}$, respectively, and read:

$$230 \quad (2.13) \quad A_i := \partial_i \ln \alpha = \frac{\partial_i \alpha}{\alpha}, \quad B_k^i := \partial_k \beta^i, \quad D_{kij} := \frac{1}{2} \partial_k \tilde{\gamma}_{ij}, \quad P_i := \partial_i \ln \phi = \frac{\partial_i \phi}{\phi}.$$

231 Hence, as a result, they must satisfy the following curl involutions or so-called second-
232 order ordering constraints [2, 68]:

$$\begin{aligned}
233 \quad & \mathcal{A}_{lk} := \partial_l A_k - \partial_k A_l = 0, \quad \mathcal{P}_{lk} := \partial_l P_k - \partial_k P_l = 0, \\
234 \quad & \mathcal{B}_{lk}^i := \partial_l B_k^i - \partial_k B_l^i = 0, \quad \mathcal{D}_{lkij} := \partial_l D_{kij} - \partial_k D_{lij} = 0.
\end{aligned}
\tag{2.14}$$

236 In the governing PDE system above, we have already made use of these curl involutions
237 by *symmetrizing* the spatial derivatives of the auxiliary variables as follows:

$$238 \quad (2.15) \quad \partial_{(k} A_{i)} := \frac{\partial_k A_i + \partial_i A_k}{2}, \quad \partial_{(k} P_{i)} := \frac{\partial_k P_i + \partial_i P_k}{2},$$

239

$$240 \quad (2.16) \quad \partial_{(k} B_{j)}^i := \frac{\partial_k B_j^i + \partial_j B_k^i}{2}, \quad \partial_{(k} D_{l)ij} := \frac{\partial_k D_{lij} + \partial_l D_{kij}}{2}.$$

241 **3. Numerical method.** In this section, we first briefly recall the standard (not
 242 well balanced) second order MUSCL-Hancock scheme applied to (2.2) and then present
 243 the novel well balanced second order finite volume scheme. Throughout this paper,
 244 we assume that the equilibria to be preserved are smooth. In other words, equilibria
 245 with jumps at the element interfaces are not admitted.

246 The one-dimensional computational domain $\Omega = [x_L, x_R]$ is covered with N uni-
 247 form segment elements of length $\Delta x = (x_R - x_L)/N$ denoted by $\Omega_i = [x_{i-1/2}, x_{i+1/2}]$,
 248 $i = 1, \dots, N$. The data at time t^n are represented by the usual cell averages \mathbf{Q}_i^n

$$249 \quad (3.1) \quad \mathbf{Q}_i^n = \frac{1}{\Delta x} \int_{\Omega_i} \mathbf{Q}(x, t^n) dx.$$

250 **3.1. Standard second-order MUSCL-Hancock-type scheme.** In the con-
 251 text of *standard* MUSCL-Hancock-type second order FV schemes [95] for PDE (2.2)
 252 the cell averages \mathbf{Q}_i^n are evolved in time from t^n up to $t^{n+1} = t^n + \Delta t$ through

$$253 \quad (3.2) \quad \begin{aligned} \mathbf{Q}_i^{n+1} = \mathbf{Q}_i^n &- \frac{\Delta t}{\Delta x} \left(\mathcal{F}_{i+\frac{1}{2}} \left(\mathbf{q}_{i+\frac{1}{2}}^-, \mathbf{q}_{i+\frac{1}{2}}^+ \right) - \mathcal{F}_{i-\frac{1}{2}} \left(\mathbf{q}_{i-\frac{1}{2}}^-, \mathbf{q}_{i-\frac{1}{2}}^+ \right) \right) \\ &- \frac{\Delta t}{\Delta x} \left(\mathcal{D}_{i-\frac{1}{2}} \left(\mathbf{q}_{i-\frac{1}{2}}^-, \mathbf{q}_{i-\frac{1}{2}}^+ \right) + \mathcal{D}_{i+\frac{1}{2}} \left(\mathbf{q}_{i+\frac{1}{2}}^-, \mathbf{q}_{i+\frac{1}{2}}^+ \right) \right) \\ &- \Delta t \mathbf{B} \left(\mathbf{q}_i^{n+\frac{1}{2}} \right) \cdot \partial_x \mathbf{Q}_i^n + \Delta t \mathbf{S} \left(\mathbf{q}_i^{n+\frac{1}{2}} \right) - \Delta t \mathbf{S}_b \left(\mathbf{q}_i^{n+\frac{1}{2}}, \partial_y \mathbf{Q}_i, \partial_z \mathbf{Q}_i \right). \end{aligned}$$

254 In (3.2), $\mathcal{F}_{i\pm\frac{1}{2}}$ represent the numerical fluxes and the $\mathcal{D}_{i\pm\frac{1}{2}}$ are the nonconserva-
 255 tive jump terms of (2.1) at the element interfaces given respectively by

$$256 \quad (3.3) \quad \mathcal{F}(\mathbf{q}^-, \mathbf{q}^+) = \frac{1}{2} (\mathbf{f}(\mathbf{q}^+) + \mathbf{f}(\mathbf{q}^-)) - \frac{1}{2} s_{\max} (\mathbf{q}^+ - \mathbf{q}^-)$$

257 and

$$258 \quad (3.4) \quad \mathcal{D}(\mathbf{q}^-, \mathbf{q}^+) = \frac{1}{2} \left(\int_0^1 \mathbf{B}_1(\Psi(\mathbf{q}^-, \mathbf{q}^+, \tau)) ds \right) \cdot (\mathbf{q}^+ - \mathbf{q}^-).$$

259 In our scheme we employ a simple Rusanov-type Riemann solver, where s_{\max} is
 260 the maximum eigenvalue of the system matrices $\mathbf{A}(\mathbf{q}^+)$ and $\mathbf{A}(\mathbf{q}^-)$, and the theory
 261 introduced in [47] is used for integrating the nonconservative products along a
 262 Lipschitz continuous path $\Psi(\mathbf{q}^-, \mathbf{q}^+, s)$ with $0 \leq s \leq 1$, $\Psi(\mathbf{q}^-, \mathbf{q}^+, 0) = \mathbf{q}^-$ and
 263 $\Psi(\mathbf{q}^-, \mathbf{q}^+, 1) = \mathbf{q}^+$. Throughout this paper we employ the simple straight-line seg-
 264 ment path

$$265 \quad (3.5) \quad \Psi(\mathbf{q}^-, \mathbf{q}^+, s) = \mathbf{q}^- + s(\mathbf{q}^+ - \mathbf{q}^-), \quad s \in [0, 1].$$

266 Moreover, in (3.2) the values

$$267 \quad (3.6) \quad \mathbf{q}_{i-\frac{1}{2}}^+ = \mathbf{q}_i^n(x_{i-\frac{1}{2}}, t^{n+\frac{1}{2}}), \quad \mathbf{q}_{i+\frac{1}{2}}^- = \mathbf{q}_i^n(x_{i+\frac{1}{2}}, t^{n+\frac{1}{2}}), \quad \mathbf{q}_i^{n+\frac{1}{2}} = \mathbf{q}_i^n(x_i, t^{n+\frac{1}{2}}),$$

268 represent the evaluation of the reconstruction polynomials $\mathbf{q}_i^n(x, t)$ respectively at
 269 the two boundaries $x_{i\pm 1/2}$ and in the barycenter x_i of Ω_i at the time-midpoint of
 270 $[t^n, t^{n+1}]$ called $t^{n+1/2}$. The reconstruction polynomial $\mathbf{q}_i^n(x, t)$ is computed through
 271 the MUSCL-Hancock strategy, see [96, 97, 95], in conjunction with the *minmod* slope

272 limiter. Thus we write it in the form of a linear polynomial in space and time that
273 reads

$$274 \quad (3.7) \quad \mathbf{q}_i^n(x, t) = \mathbf{w}_i^n(x, t^n) + \partial_t \mathbf{Q}_i^n(t - t^n), \quad \text{with } \mathbf{w}_i^n(x, t^n) = \mathbf{Q}_i^n + \partial_x \mathbf{Q}_i^n(x - x_i).$$

275 In the above formula the spatial gradient is given by

$$276 \quad (3.8) \quad \partial_x \mathbf{Q}_i^n = \text{minmod} \left(\frac{\Delta \mathbf{Q}_{i+\frac{1}{2}}^n}{\Delta x}, \frac{\Delta \mathbf{Q}_{i-\frac{1}{2}}^n}{\Delta x} \right),$$

277 with the jumps $\Delta \mathbf{Q}_{i-\frac{1}{2}}^n = \mathbf{Q}_i^n - \mathbf{Q}_{i-1}^n$ and $\Delta \mathbf{Q}_{i+\frac{1}{2}}^n = \mathbf{Q}_{i+1}^n - \mathbf{Q}_i^n$ across the left and
278 the right cell boundary respectively, and the usual minmod function

$$279 \quad (3.9) \quad \text{minmod}(a, b) = \begin{cases} 0, & \text{if } ab \leq 0, \\ a, & \text{if } |a| < |b|, \\ b, & \text{if } |a| \geq |b|. \end{cases}$$

280 The term $\partial_t \mathbf{Q}_i^n$ indicates the approximation of the time derivative of \mathbf{Q} and is com-
281 puted using a discrete version of the governing equation

$$282 \quad \partial_t \mathbf{Q}_i^n = - \frac{\mathbf{f}(\mathbf{Q}_i^n + \frac{1}{2} \Delta x \partial_x \mathbf{Q}_i^n) - \mathbf{f}(\mathbf{Q}_i^n - \frac{1}{2} \Delta x \partial_x \mathbf{Q}_i^n)}{\Delta x} \\ 283 \quad (3.10) \quad + \mathbf{S}(\mathbf{Q}_i^n) - \mathbf{S}_b(\mathbf{Q}_i^n, \partial_y \mathbf{Q}_i, \partial_z \mathbf{Q}_i) - \mathbf{B}_1(\mathbf{Q}_i^n) \cdot \partial_x \mathbf{Q}_i^n.$$

284 Since we are working in the one-dimensional framework of (2.2), only the first
285 component of the gradient of \mathbf{Q} , i.e. $\partial_x \mathbf{Q}_i^n$ needs to be computed in each time step
286 according to (3.8). Instead, $\partial_y \mathbf{Q}_i$ and $\partial_z \mathbf{Q}_i$ are assumed to be known functions that
287 are constant in time. Depending on the test problem, they may be non-zero. When
288 not analytically available, they are computed once at the beginning of the simulation
289 using a fourth order accurate finite difference approximation. Finally, the time step
290 Δt is chosen according to a CFL condition

$$291 \quad (3.11) \quad \Delta t = \text{CFL} \min_{\Omega_i} \frac{\Delta x}{|\lambda_{\max, i}|}, \quad \forall \Omega_i \in \Omega,$$

292 where the Courant-Friedrichs-Levy number is set to $\text{CFL} < 1$ and $|\lambda_{\max, i}|$ is the
293 maximum absolute value of the eigenvalues in the cell Ω_i .

294 **3.2. Well balanced second order FV scheme.** The scheme (3.2) and the
295 above reconstruction procedure can be made well balanced by adopting the strategy
296 first proposed in [80, 37, 38] and further developed for smooth equilibrium profiles
297 in [21, 67, 40]. The fundamental idea consists in exploiting the knowledge of the
298 equilibrium profile $\mathbf{Q}^E(x)$ that needs to be preserved in order to rewrite (3.2) as
299 follows

$$300 \quad (3.12) \quad \mathbf{Q}_i^{n+1} = \mathbf{Q}_i^n - \frac{\Delta t}{\Delta x} \left[\left(\mathcal{F}_{i+\frac{1}{2}} \left(\mathbf{q}_{i+\frac{1}{2}}^-, \mathbf{q}_{i+\frac{1}{2}}^+ \right) - \mathbf{f}(\mathbf{Q}_{i+\frac{1}{2}}^E) \right) + \mathcal{D}_{i+\frac{1}{2}} \left(\mathbf{q}_{i+\frac{1}{2}}^-, \mathbf{q}_{i+\frac{1}{2}}^+ \right) \right. \\ \left. - \left(\mathcal{F}_{i-\frac{1}{2}} \left(\mathbf{q}_{i-\frac{1}{2}}^-, \mathbf{q}_{i-\frac{1}{2}}^+ \right) - \mathbf{f}(\mathbf{Q}_{i-\frac{1}{2}}^E) \right) + \mathcal{D}_{i-\frac{1}{2}} \left(\mathbf{q}_{i-\frac{1}{2}}^-, \mathbf{q}_{i-\frac{1}{2}}^+ \right) \right] \\ - \Delta t \left(\mathbf{B} \left(\mathbf{q}_i^{n+\frac{1}{2}} \right) \partial_x \mathbf{Q}_i^n - \mathbf{B} \left(\mathbf{Q}_i^E \right) \partial_x \mathbf{Q}_i^E \right) + \Delta t \left(\mathbf{S} \left(\mathbf{q}_i^{n+\frac{1}{2}} \right) - \mathbf{S} \left(\mathbf{Q}_i^E \right) \right) \\ - \Delta t \left(\mathbf{S}_b \left(\mathbf{q}_i^{n+\frac{1}{2}}, \partial_y \mathbf{Q}_i, \partial_z \mathbf{Q}_i \right) - \mathbf{S}_b \left(\mathbf{Q}_i^E, \partial_y \mathbf{Q}_i^E, \partial_z \mathbf{Q}_i^E \right) \right).$$

301 The *validity* of (3.12) can be easily *justified* by first noticing that
 302

$$303 \quad (3.13) \quad \frac{\mathbf{f}(\mathbf{Q}_{i+\frac{1}{2}}^E) - \mathbf{f}(\mathbf{Q}_{i-\frac{1}{2}}^E)}{\Delta x} + \frac{1}{\Delta x} \int_{\Omega_i} \left[\mathbf{B}_1(\mathbf{Q}^E) \partial_x \mathbf{Q}^E + \mathbf{S}(\mathbf{Q}^E) \right. \\ \left. - \mathbf{S}_b(\mathbf{Q}^E, \partial_y \mathbf{Q}^E, \partial_z \mathbf{Q}^E) \right] dx$$

304
 305
 306 is *exactly zero* by construction, since it coincides with the PDE system (2.2) evaluated
 307 at the equilibrium. Then, by subtracting (3.13) to the standard non well balanced
 308 FV solver (3.2) and using the midpoint rule to approximate the integrals in (3.13), we
 309 get exactly (3.12). As discussed later, for $\mathbf{q}_i(x, t) = \mathbf{Q}_i^E(x)$ one immediately obtains
 310 $\mathbf{Q}_i^{n+1} = \mathbf{Q}_i^n$ from (3.12), independently of the quadrature rules employed in (3.13),
 311 since all differences of the numerical solution with respect to the equilibrium solution
 312 in (3.12) cancel. For the sake of completeness, we recall that in (3.12)

$$313 \quad (3.14) \quad \mathbf{Q}_{i\pm\frac{1}{2}}^E = \mathbf{Q}^E(x_{i\pm\frac{1}{2}}), \quad \mathbf{Q}_i^E = \mathbf{Q}^E(x_i)$$

314 and

$$315 \quad (3.15) \quad \partial_x \mathbf{Q}_i^E = \frac{\mathbf{Q}_{i+\frac{1}{2}}^E - \mathbf{Q}_{i-\frac{1}{2}}^E}{\Delta x}, \quad \partial_x \mathbf{Q}_i^n = \partial_x \mathbf{Q}_i^E + \partial_x \mathbf{Q}_i^{f,n},$$

316 where $\mathbf{Q}_i^{f,n}$ is given in (3.18). Finally, $\partial_y \mathbf{Q}_i^E$ and $\partial_z \mathbf{Q}_i^E$ are computed using the same
 317 procedure as the one employed for $\partial_y \mathbf{Q}_i$ and $\partial_z \mathbf{Q}_i$.

318 A similar scheme could be derived following the strategy described in in [62],
 319 where a special path is defined to achieve the well balanced property, indeed in that
 320 case the proposed path was composed of two components

$$321 \quad (3.16) \quad \Phi(s, \mathbf{q}^-, \mathbf{q}^+) = \Phi^E(s, \mathbf{q}_E^-, \mathbf{q}_E^+) + \Phi^f(s, \mathbf{q}_f^-, \mathbf{q}_f^+),$$

322 where $\Phi^E(s, \mathbf{q}_E^-, \mathbf{q}_E^+)$ is a re-parametrization of the equilibrium solution of interest that
 323 connects the two equilibrium states \mathbf{q}_E^- and \mathbf{q}_E^+ with each other, and $\Phi^f(s, \mathbf{q}_f^-, \mathbf{q}_f^+) =$
 324 $\mathbf{q}_f^- + s(\mathbf{q}_f^+ - \mathbf{q}_f^-)$ is a standard segment path but acting *only* on the *fluctuations*
 325 with respect to \mathbf{q}_E , defined as $\mathbf{q}_f^- = \mathbf{q}^- - \mathbf{q}_E^-$ and $\mathbf{q}_f^+ = \mathbf{q}^+ - \mathbf{q}_E^+$, respectively.
 326 Here, the fact of computing separately the contributions coming from the equilibrium
 327 components of the solution and subtracting them pointwise allows to immediately
 328 cancel the numerical errors introduced in that part of the computation and allows an
 329 increased resolution on the fluctuations with respect to that equilibrium.

330 Also the reconstruction procedure (3.7) is modified according to the strategy pro-
 331 posed in [38] that consists in reconstructing only the fluctuations w.r.t the equilibrium
 332 and summing up the exact equilibrium value. This gives

$$333 \quad (3.17) \quad \mathbf{q}_i^n(x, t) = \mathbf{Q}_i^E(x) + \mathbf{w}_i^{f,n}(x, t) + \partial_t \mathbf{Q}_i^{f,n}(t - t^n), \quad \text{with} \\ \mathbf{w}_i^{f,n}(x, t) = \mathbf{Q}_i^{f,n} + \partial_x \mathbf{Q}_i^{f,n}(x - x_i),$$

334 where $\mathbf{w}_i^{f,n}$ and $\partial_t \mathbf{Q}_i^{f,n}$ are respectively obtained with (3.8) and (3.10), but applied
 335 to the fluctuations $\mathbf{Q}_i^{f,n} = \mathbf{Q}_i^n - \mathbf{Q}_i^E$ around the equilibrium, i.e.

$$336 \quad (3.18) \quad \partial_x \mathbf{Q}_i^{f,n} = \text{minmod} \left(\frac{\mathbf{Q}_{i+1}^{f,n} - \mathbf{Q}_i^{f,n}}{\Delta x}, \frac{\mathbf{Q}_i^{f,n} - \mathbf{Q}_{i-1}^{f,n}}{\Delta x} \right);$$

337 finally, for what concerns the time evolution $\partial_t \mathbf{Q}_i^{f,n}$, it is again recovered from a
 338 discrete version of the governing PDE (2.2) evaluated at the reconstructed values
 339 minus the same PDE evaluated at the equilibrium, i.e.

$$\begin{aligned}
 \partial_t \mathbf{Q}_i^{f,n} = & -\frac{1}{\Delta x} \left[\left(\mathbf{f} \left(\mathbf{Q}_i^E(x_{i+\frac{1}{2}}) + \mathbf{w}_i^{f,n}(x_{i+\frac{1}{2}}, t) \right) - \mathbf{f} \left(\mathbf{Q}_i^E(x_{i+\frac{1}{2}}) \right) \right) \right. \\
 (3.19) \quad & \left. - \left(\mathbf{f} \left(\mathbf{Q}_i^E(x_{i-\frac{1}{2}}) + \mathbf{w}_i^{f,n}(x_{i-\frac{1}{2}}, t) \right) - \mathbf{f} \left(\mathbf{Q}_i^E(x_{i-\frac{1}{2}}) \right) \right) \right] \\
 & + \mathbf{S}(\mathbf{Q}_i^n) - \mathbf{S}(\mathbf{Q}_i^E) - \mathbf{S}_b(\mathbf{Q}_i^n, \partial_y \mathbf{Q}_i, \partial_z \mathbf{Q}_i) + \mathbf{S}_b(\mathbf{Q}_i^E, \partial_y \mathbf{Q}_i^E, \partial_z \mathbf{Q}_i^E) \\
 & - \mathbf{B}_1(\mathbf{Q}_i^n) \cdot \partial_x \mathbf{Q}_i^n + \mathbf{B}_1(\mathbf{Q}_i^E) \cdot \partial_x \mathbf{Q}_i^E.
 \end{aligned}$$

341

342 Finally, it is trivial to *prove* that the scheme (3.12) associated with the recon-
 343 struction procedure (3.17) with the definitions (3.14) and (3.15), is well balanced for
 344 any smooth equilibrium $\mathbf{Q}^E(x)$. Indeed, if the initial condition coincides with the
 345 chosen equilibrium, i.e $\mathbf{Q}_i^0 = \mathbf{Q}^E(x_i)$, then at each timestep the fluctuations will be
 346 automatically zero and the reconstruction polynomial will be set equal to the equi-
 347 librium $\mathbf{q}(x, t) = \mathbf{Q}^E(x)$, according to (3.17). At this point each term of (3.12)
 348 cancels exactly, and $\mathbf{Q}_i^{n+1} = \mathbf{Q}_i^n = \mathbf{Q}_i^E$ for any cell Ω_i of the domain. It should
 349 be underlined that this proof is particularly simple due to the fact that the equi-
 350 libria under consideration are smooth, $\mathbf{q}_{i\pm\frac{1}{2}}^- = \mathbf{q}_{i\pm\frac{1}{2}}^+ = \mathbf{Q}_{i\pm\frac{1}{2}}^E$, and the numerical
 351 flux $\mathcal{F}_{i\pm\frac{1}{2}}(\mathbf{q}_{i\pm\frac{1}{2}}^-, \mathbf{q}_{i\pm\frac{1}{2}}^+) = \mathbf{f}(\mathbf{Q}_{i\pm\frac{1}{2}}^E)$. We furthermore remark that the well balanced
 352 scheme (3.12) will behave as the standard scheme (3.2) when \mathbf{Q}_i^n is far away from the
 353 chosen equilibria.

354 **4. Numerical results.** In this section, we show the increased resolution and
 355 stability of our second order well balanced finite volume method (3.12) with respect
 356 to a standard not well balanced second order scheme (3.2) for two typical applications
 357 in general relativity, namely the Michel-Bondi accretion disk (Section 4.1) and the
 358 TOV neutron star (Section 4.3). The considered problems are all characterized by
 359 a spherical symmetry, so in order to ease the comprehension we adopt the following
 360 notation $\mathbf{x} = (x_1, x_2, x_3) = (r, \theta, \phi)$.

361 We proceed as follows: after verifying that for an equilibrium initial condition
 362 $\mathbf{Q}(\mathbf{x}, 0) = \mathbf{Q}^E(\mathbf{x})$ the new well balanced scheme is always exact up to machine preci-
 363 sion, we test the performance of the well balanced algorithm and a classical not well
 364 balanced method on initial conditions that could be considered as perturbations of
 365 the chosen equilibrium. As expected, for large perturbations the two schemes behave
 366 practically the same, while for small perturbations (which are indeed the target of this
 367 work) the WB method is more accurate and more stable, hence allowing much longer
 368 simulations compared to a standard scheme. In particular, for what concerns the
 369 TOV star, we first study i) the *evolution of the matter* via the GRMHD system when
 370 subject to a pressure perturbation on a *fixed* background space-time *metric* (Cowling
 371 approximation, see Section 4.3.2), then ii) the *evolution* of the space-time *metric*,
 372 subject to a perturbation of the extrinsic curvature, but assuming the *matter* vari-
 373 ables as externally given and *fixed* (anti-Cowling approximation, see Section 4.3.3),
 374 and finally iii) the *fully coupled evolution of matter and metric* when subject to either
 375 a pressure or a space-time perturbation (see Section 4.3.4).

376 Finally, for the sake of completeness, we also verify numerically the order of
 377 convergence of the employed well balanced scheme, see Section 4.4.

378 **4.1. Michel accretion disk.** As first test case we consider a smooth flow with
 379 an analytical solution on a curved space–time: it consists in the stationary spherical
 380 transonic accretion of an isentropic fluid onto a non-rotating black hole and it is known
 381 as *Michel-Bondi* solution [76]. The explicit expressions of the lapse, the shift and the
 382 spatial metric of a Kerr black hole with mass M and spin a in the employed spherical
 383 Kerr-Schild (KS) coordinates (r, θ, ϕ) are given by [73]

$$384 \quad (4.1) \quad \alpha = (1+z)^{-\frac{1}{2}}, \quad \beta^i = \left(\frac{z}{1+z}, 0, 0 \right),$$

$$\gamma_{ij} = \begin{pmatrix} 1+z & 0 & -a \sin^2 \theta (1+z) \\ 0 & \rho^2 & 0 \\ -a \sin^2 \theta (1+z) & 0 & \Sigma \sin^2 \theta / \rho^2 \end{pmatrix},$$

385 with

$$386 \quad (4.2) \quad \rho^2 = r^2 + a^2 \cos^2 \theta, \quad z = \frac{2r}{\rho^2},$$

$$\Delta = r^2 + a^2 - 2Mr, \quad \Sigma = (r^2 + a^2)^2 - a^2 \Delta \sin^2 \theta.$$

387 By considering this metric with $a = 0$ and by fixing the mass $M = 1$, the critical radius
 388 $r_c = 8M$ and the critical density $\rho_c M^2 = 1/16$, the Michel equilibrium solution $\mathbf{Q}^E(r)$
 389 can be determined analytically, see for example [86]. This test is performed with the
 390 so-called Cowling approximation, i.e. the background space-time is assumed to be
 391 fixed. We perform this test on a spatial 1D domain Ω with $r \in [1.5, 10.5]$, $\theta = \pi/2$ and
 392 $\phi = 0$, discretized with $N = 100$ intervals and evolved up to the final time $t_f = 10^5$.
 393 We have first verified that for an initial condition equal to the equilibrium $\mathbf{Q}^E(r)$ the
 394 WB scheme does not exhibit any numerical errors, and then we have perturbed the
 395 initial condition by adding a Gaussian bump to the equilibrium pressure profile as

$$396 \quad (4.3) \quad p = p^E + 10^{-3} \exp\left(-0.5 \frac{(r-5)^2}{0.5^2}\right)$$

397 (see the left image of Figure 1). The numerical results obtained with the new WB
 398 scheme and with a standard second order not well balanced scheme are reported in
 399 Figure 1 and show how the WB scheme is able to recover the equilibrium profile once
 400 the bump has exited the domain, while this is not the case for the not WB scheme.

401 **4.2. Solution of a Riemann problem with prescribed Michel equilib-**
 402 **rium.** We choose the second test case in order to show numerically that the WB
 403 property of the scheme, which radically improves its resolution near the equilibria,
 404 does not affect negatively any capability of the underlying second order scheme when
 405 performing simulations far away from the chosen equilibrium. Thus, while choosing
 406 as equilibrium the Michel solution over the KS coordinates described in the previous
 407 Section 4.1, we use our schemes to solve the following Riemann problem [57]

$$408 \quad (4.4) \quad (\rho, \mathbf{u}, p, \mathbf{B}) = \begin{cases} (0.125, \mathbf{0}, 0.1, \mathbf{0}) & \text{if } r \leq 4 \\ (1, \mathbf{0}, 1, \mathbf{0}) & \text{if } r > 4 \end{cases}$$

409 over a flat Minkowski space–time, that is $\alpha = 1$, $\beta^i = (0, 0, 0)$ and $\gamma_{ij} = \mathbf{I}$, on
 410 a spatial 1D domain Ω with $x_1 \in [2, 6]$. Note that, even if the initial condition
 411 completely differs both for matter and metric from the chosen equilibrium, the WB
 412 scheme is able to return the same results of the not WB scheme, see Figure 2. Indeed
 413 far from the equilibrium the two schemes are both nominally second order accurate
 414 shock capturing TVD schemes and are expected to return equally accurate results.

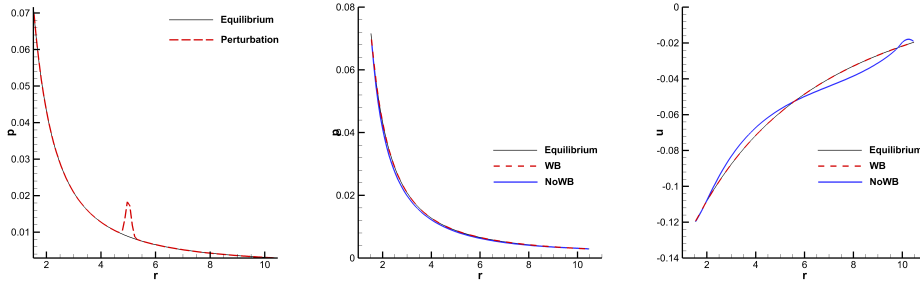


FIG. 1. Michel accretion disk, equilibrium solution of GRMHD. We show the equilibrium profile (continuous black line) for pressure (left, middle) and velocity (right), and the initial perturbed pressure condition (red dashed line, left). Then, in the middle and right panels we report the numerical results obtained at time $t_f = 10^5$ with the well balanced scheme (dashed red lines) and the not well balanced scheme (continuous blue lines). We remark that the initial bump is expected to split into two waves traveling out of the domain so that after a long simulation time the equilibrium profile should be recovered: this is the case with the WB scheme while the not WB scheme destroys the equilibrium profile (note in particular the completely unstable velocity profile, right panel).

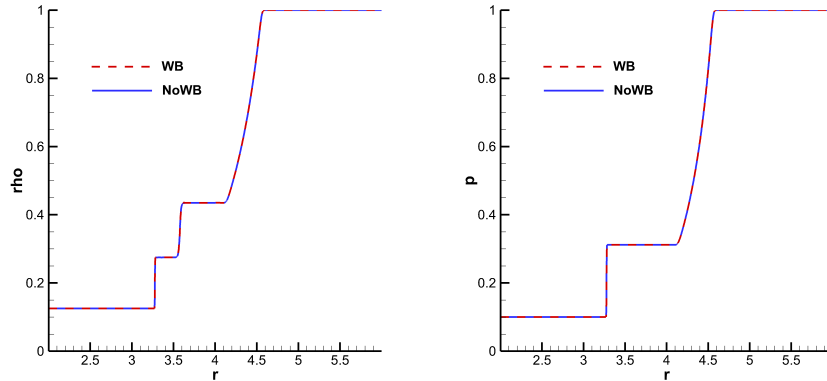


FIG. 2. GRMHD Riemann problem. We show the numerical results for the density (left) and the pressure (right) obtained with a standard not WB scheme (blue) which coincide with those obtained with the new WB scheme (red) although the latter is set to maintain the Michel equilibrium.

415 **4.3. TOV Neutron star.** The next phenomenon that we want to investigate is
 416 the long time evolution of a stable Tolman-Oppenheimer-Volkoff (TOV) neutron star
 417 and the effects of small perturbations of metric and matter variables on the entire
 418 system. For the details on the derivation of the radially symmetric TOV solution, we
 419 refer to [94, 78, 98, 36, 34].

420 In the following, we will consider three different situations, namely the matter
 421 evolution on a fixed space-time metric through the GRMHD model (Cowling approx-
 422 imation), the space-time metric evolution in the anti-Cowling approximation through
 423 the FO-CCZ4 model, and the fully coupled evolution of metric and matter through
 424 the combined FO-CCZ4+GRMHD model. In the three cases we run the test problem
 425 on a 1D domain Ω with $r \in [0.5, 14]$, $\theta = \pi/2$, $\phi = 0$ discretized with $N = 1000$
 426 intervals.

427 To impose the *boundary conditions* we proceed as follows. First, we use one ghost

428 cell at each boundary set on the equilibrium value \mathbf{Q}^E . Next, we define a left and a
 429 right sponge layer $\mathcal{S}_{\mathcal{L},\mathcal{R}}$ (see also [18]) so that

$$430 \quad (4.5) \quad x \in \mathcal{S}_{\mathcal{L},\mathcal{R}} \quad \text{if} \quad |x - x_{L,R}| < s_{\mathcal{L},\mathcal{R}}$$

431 on which the numerical solution is redefined as

$$432 \quad (4.6) \quad \tilde{\mathbf{q}} = (1 - \varepsilon_{L,R})\mathbf{q}_h + \varepsilon_{L,R}\mathbf{Q}^E.$$

433 These conditions are employed to impose an absorbing boundary condition which
 434 reduces the reflection of waves, and allows in particular the numerical errors traveling
 435 through the cleaning variables (as θ in the FO-CCZ4 model) to exit the domain.

436 To check the *validity* of the obtained numerical results we will monitor i) the
 437 profile of the solution, ii) the oscillation of the mass density at the center of the star,
 438 and iii) the temporal evolution of the Hamiltonian and momentum constraints, which
 439 are nonlinear elliptic involutions (hence not containing time derivatives) that should
 440 be satisfied everywhere

$$441 \quad (4.7) \quad \begin{aligned} \mathcal{H} &= R_{ij}g^{ij} - K_{ij}K^{ij} + K^2 - 16\pi\tau = 0, \\ \mathcal{M}_i &= \gamma^{jl} (\partial_l K_{ij} - \partial_i K_{jl} - \Gamma_{jl}^m K_{mi} + \Gamma_{ji}^m K_{ml}) - 8\pi S_i = 0. \end{aligned}$$

442 At this point, we would like to remark that the TOV equilibrium solution is not
 443 available in the form of an analytical expression, but just as the numerical solution
 444 of a system of four ODEs (see [34] for example). Because of that, already the initial
 445 equilibrium condition does not satisfy exactly (4.7). Our aim will be thus preserving
 446 constantly the initial values of \mathcal{H} and \mathcal{M}_i .

447 Finally, we emphasize that when the imposed initial conditions coincide exactly
 448 with the TOV equilibrium, the WB scheme is able to preserve it *indefinitely* without
 449 the introduction of any numerical errors and to perfectly maintain constants the values
 450 of the constraints. This well balanced property of our algorithm is further numerically
 451 verified in Section 4.3.1.

452

453 4.3.1. Numerical proof of the well balanced property of our algorithm.

454 First of all, in order to present a numerical proof of the well balanced capabilities of
 455 the proposed second order well balanced scheme we have set up the following test.

456 Usually one claims that this property is verified when an equilibrium initial con-
 457 dition is preserved with machine accuracy for very long computational times. For
 458 our well balanced scheme this is trivially verified for any smooth equilibrium initial
 459 conditions $\mathbf{Q}(x, 0)$ taken equal to the equilibrium profile \mathbf{Q}^E to be preserved. Since
 460 no numerical errors are introduced by the scheme, this property can be easily verified
 461 also numerically.

462 To make this test more challenging and convincing, we have added a small ran-
 463 dom perturbation of the order of machine accuracy to the initial equilibrium profiles
 464 and we have monitored its evolution working in *single*, *double* and *quadruple* preci-
 465 sion. We have applied this approach for all the equilibrium profiles presented in this
 466 paper. In particular, we have modified the density and the pressure when employing
 467 the GRMHD equations, and the trace of the extrinsic curvature K when using the
 468 FO-CCZ4 system or the fully coupled approach, with random perturbations of the
 469 order of the corresponding machine precision used for the simulations. In Table 1 we
 470 have reported the numerical errors with respect to the equilibrium profiles for several
 471 variables of interest at short and long simulation times. In all the cases the numerical
 472 errors remain of the order of machine precision.

TABLE 1

Numerical proof of the well balanced property of the new well balanced finite volume scheme presented in this paper, as described in Section 4.3.1.

Precision Time	Single				Double				Quadruple			
	Δt	1	100	1000	Δt	1	100	1000	Δt	1	100	1000
Michel												
ρ	1E-07	8E-08	7E-08	9E-08	2E-14	2E-14	4E-14	4E-14	1E-28	1E-28	5E-29	1E-31
p	2E-07	2E-07	2E-07	2E-07	1E-14	1E-14	1E-14	1E-14	1E-28	2E-28	1E-29	1E-32
TOV GRMHD												
ρ	2E-07	3E-06	1E-05	1E-05	2E-14	7E-13	3E-12	2E-12	2E-28	7E-27	3E-26	2E-26
p	2E-07	2E-07	5E-07	2E-07	2E-14	2E-14	4E-14	5E-14	2E-28	2E-28	4E-28	3E-28
TOV anti-Cowling												
K	2E-07	2E-07	3E-07	5E-07	2E-14	2E-14	5E-14	7E-14	2E-28	2E-28	2E-28	6E-28
θ	0	5E-09	7E-09	7E-09	4E-19	6E-15	1E-14	4E-14	2E-33	4E-30	2E-28	2E-27
TOV fully coupled												
ρ	0	1E-14	1E-07	9E-06	0	1E-19	4E-15	5E-14	0	2E-31	1E-29	4E-30
K	2E-07	2E-07	8E-06	9E-06	2E-14	2E-14	8E-15	4E-14	2E-28	2E-28	1E-28	9E-30
θ	1E-11	5E-08	5E-06	9E-06	3E-19	2E-15	9E-15	3E-14	1E-32	1E-30	4E-29	7E-30
γ_{11}	0	0	1E-05	2E-05	2E-18	2E-15	5E-15	3E-14	0	1E-31	1E-29	2E-29

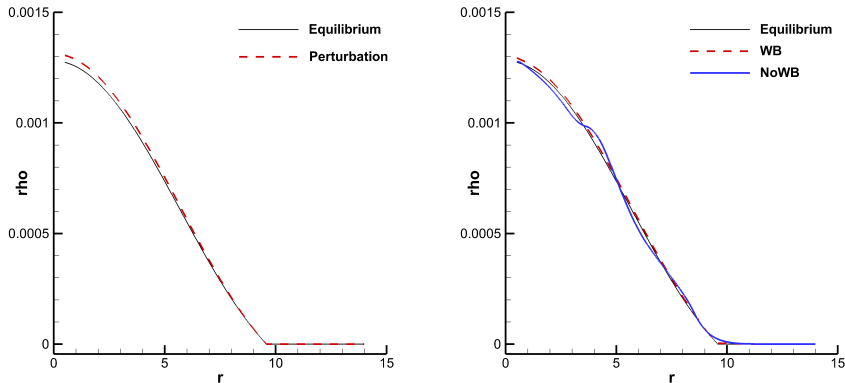


FIG. 3. GRMHD TOV star simulation. We show the initial pressure perturbed profile (left) and the comparison between the equilibrium profile and the numerical results obtained with the new WB and the not WB schemes at the final time $t_f = 10000$ (right). Note that only the WB algorithm is able to preserve the shape of the equilibrium over long computational times.

473 **4.3.2. TOV neutron star simulated with the GRMHD system in Cowling**
 474 **approximation.** Using the GRMHD system we can simulate the evolution of
 475 the TOV neutron star on a fixed space–time metric. In particular, we have perturbed
 476 the initial equilibrium pressure profile as follows

$$477 \quad (4.8) \quad p = (1.0 + 0.05)p^E \quad \forall \mathbf{x} \text{ in } \Omega,$$

478 which results also in a density perturbation, being $\rho = (p/\kappa)^{1/\gamma}$, see the left panel of
 479 Figure 3. For what concerns the sponge layer, we have activated it only for the right
 480 boundary, i.e we choose $s_{\mathcal{L}} = 0$, $s_{\mathcal{R}} = 3$ and $\varepsilon_R = 10^{-4}$. This allows to see the mass
 481 oscillations at the center of the star, see Figure 4.

482 The simulation has been run with the new WB scheme and with a standard
 483 second order not WB method. The obtained results at the final time $t_f = 10000$ are
 484 presented in Figure 3 and they show that after long simulation times the WB scheme
 485 is still able to maintain the expected profile of the solution perfectly well, while the
 486 not WB scheme is strongly affected by the accumulation of numerical errors.

487 **4.3.3. TOV neutron star simulated with FO-CCZ4 in the anti-Cowling**
 488 **approximation.** Next, we consider the evolution of the space–time metric in the
 489 anti-Cowling approximation, i.e. we assume the matter quantities to be *stationary* in
 490 time and externally given by the Tolman–Oppenheimer–Volkoff (TOV) solution.

491 As gauge conditions we employ a frozen shift condition $\partial_t \beta^i = 0$ by setting $s = 0$
 492 in the FO-CCZ4 system, together with the harmonic slicing, which corresponds to
 493 the choice $g(\alpha) = 1$. The cleaning speed for the cleaning of the nonlinear ADM
 494 constraints is set to $e = 1.5$. The remaining constants in the FO-CCZ4 system are
 495 chosen as $\gamma = 1.4$, $\kappa_1 = \kappa_2 = \kappa_3 = 0$, $c = 0$ and $\eta = 0$.

496 We study here the effects of an initial perturbation over the variable K so that

$$497 \quad (4.9) \quad K(r, 0) = K^E(r) + 10^{-5} \exp\left(-0.5 \frac{(r - 6.0)^2}{0.1^2}\right),$$

498 see also the left panel of Figure 5. The bump should split into two waves which
 499 are expected to propagate until exiting the domain. This happens when using the

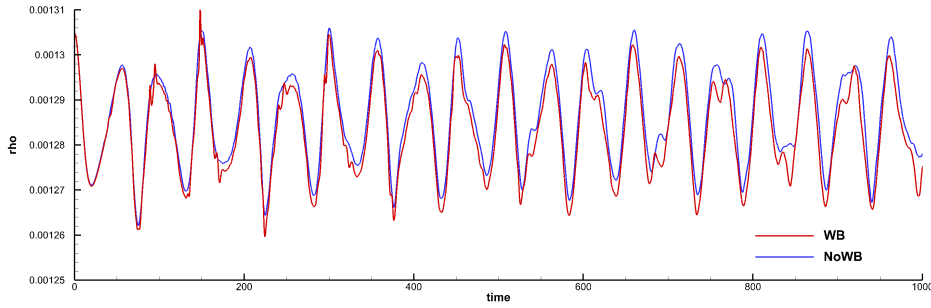


FIG. 4. GRMHD TOV star simulation. We show the oscillating density of the TOV star at an inner point with $r = 0.5$ over $t \in [0, 1000]$ obtained with the new WB and the not WB second order schemes.

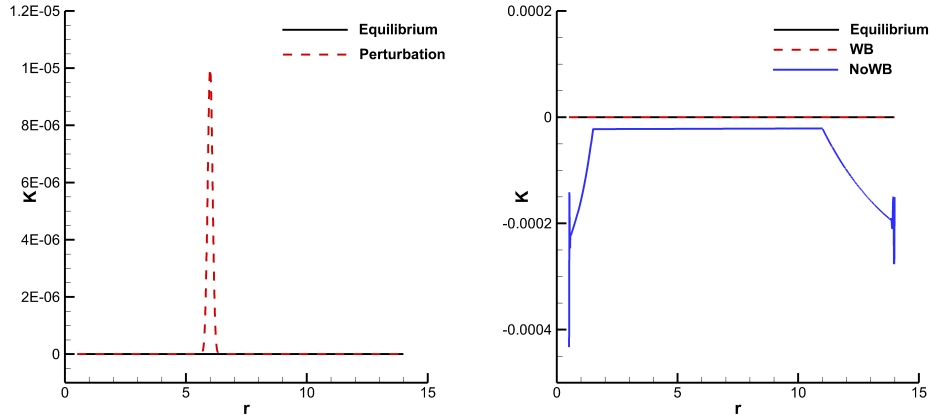


FIG. 5. TOV star simulation in anti-Cowling approximation. We show the initial perturbed profile of the metric variable K (left) and the comparison between the equilibrium profile and the numerical results obtained with the new WB and the not WB methods at the final time $t_f = 1000$ (right). Note that the WB algorithm let the perturbation exit the domain and K recovers its equilibrium profile while the not WB code corrupts the simulation. We underline that the error on the K profile with the WB code are of the order of 10^{-9} .

500 WB scheme where indeed the equilibrium profile of K is soon recovered (with an
 501 error of 10^{-9} at the final time $t_f = 1000$) while with a not WB scheme the presence
 502 of numerical errors prevents the restoring of the equilibrium, see the right panel of
 503 Figure 5. For what concerns the sponge layer, we choose $s_{\mathcal{L}} = 1.0$, $s_{\mathcal{R}} = 3$, $\varepsilon_L = 10^{-3}$
 504 and $\varepsilon_R = 10^{-4}$ to avoid the spurious reflection of waves at the boundaries.

505 Finally, we monitor the Hamiltonian and momentum constraints (4.7) over the
 506 time, refer to Figure 6. Since the initial perturbed profile of K (4.9) does not sat-
 507 isfy the equations we can notice a higher peak at the beginning of the simulation.
 508 Then, once the perturbation has exited the domain, the WB scheme is able to recover
 509 constraint values closer to zero w.r.t to the not WB scheme.

510 **4.3.4. TOV neutron star simulated with the fully coupled FO-CCZ4 +**
 511 **GRHD model.** Finally, we consider the fully coupled model that can be obtained by
 512 considering together the FO-CCZ4 model and the GRMHD model; the initial metric
 513 values and the parameters for the ADM constraints are set as in the previous test case.

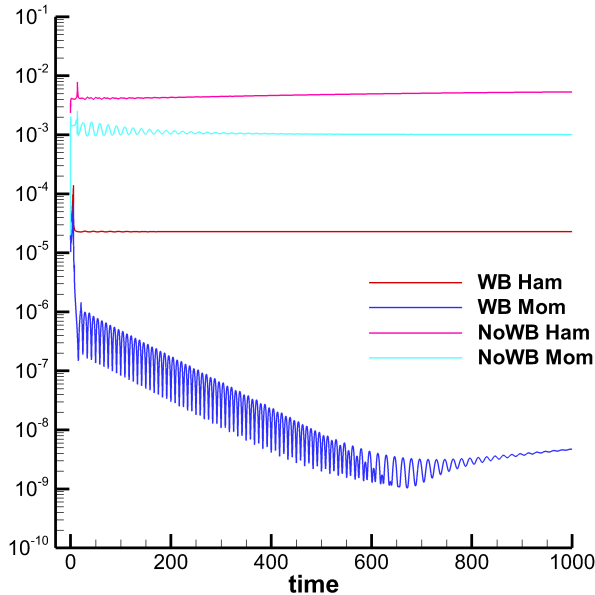


FIG. 6. Hamiltonian (*Ham*) and momentum (*Mom*) constraints for the TOV star simulation in anti-Cowling approximation over the time $t \in [0, 1000]$. Note i) the initial pick due to the fact that the initial perturbed profile of K does not satisfy the equations, ii) the more closer to machine precision values obtained with the WB schemes for both the constraints, iii) the decreasing/slightly increasing behaviors of the constraints obtained with the WB/not WB codes.

514 In what follows we study two different perturbations of the stationary TOV neutron
 515 star profile. We would like to remark that, up to our knowledge, these are the *first*
 516 numerical simulations ever presented with a well balanced finite volume scheme for
 517 the fully coupled Einstein-Euler system. Long time stability is achieved thanks to the
 518 use of the novel WB techniques, which are able to stabilize the simulation and avoid
 519 the accumulation of spurious numerical errors.

520 **Perturbation of the metric variable K .** First, we perturb the initial value of
 521 the metric variable K as in (4.9) and for what concerns the sponge layer, we choose
 522 $s_{\mathcal{L}} = 1.0$, $s_{\mathcal{R}} = 3$, $\varepsilon_L = 10^{-3}$ and $\varepsilon_R = 10^{-4}$.

523 We report in Figure 7 the profile of some metric variables and in Figure 8 the
 524 profile of the density and pressure in the matter. These results have been obtained
 525 on one hand by using the new WB scheme presented in this paper, which allows to
 526 recover and maintain the equilibrium profile even for very long simulation times of
 527 $t = 1000$ or $t = 5000$, and on the other hand with a standard second order scheme
 528 that, even on a four times finer mesh completely destroys the solution profile in a
 529 time of only $t = 50$.

530 The difference in resolution and stability between the WB and not WB scheme is
 531 made evident also by the monitoring of the Hamiltonian and momentum constraints,
 532 see Figure 9: right from the beginning, the WB scheme allows a much more precise
 533 representation of the discrete solution and consequently also the errors in the invo-
 534 lution constraints are much lower; moreover, these smaller values of \mathcal{H} and \mathcal{M} are
 535 almost constantly maintained in time by the WB scheme, while their values explode

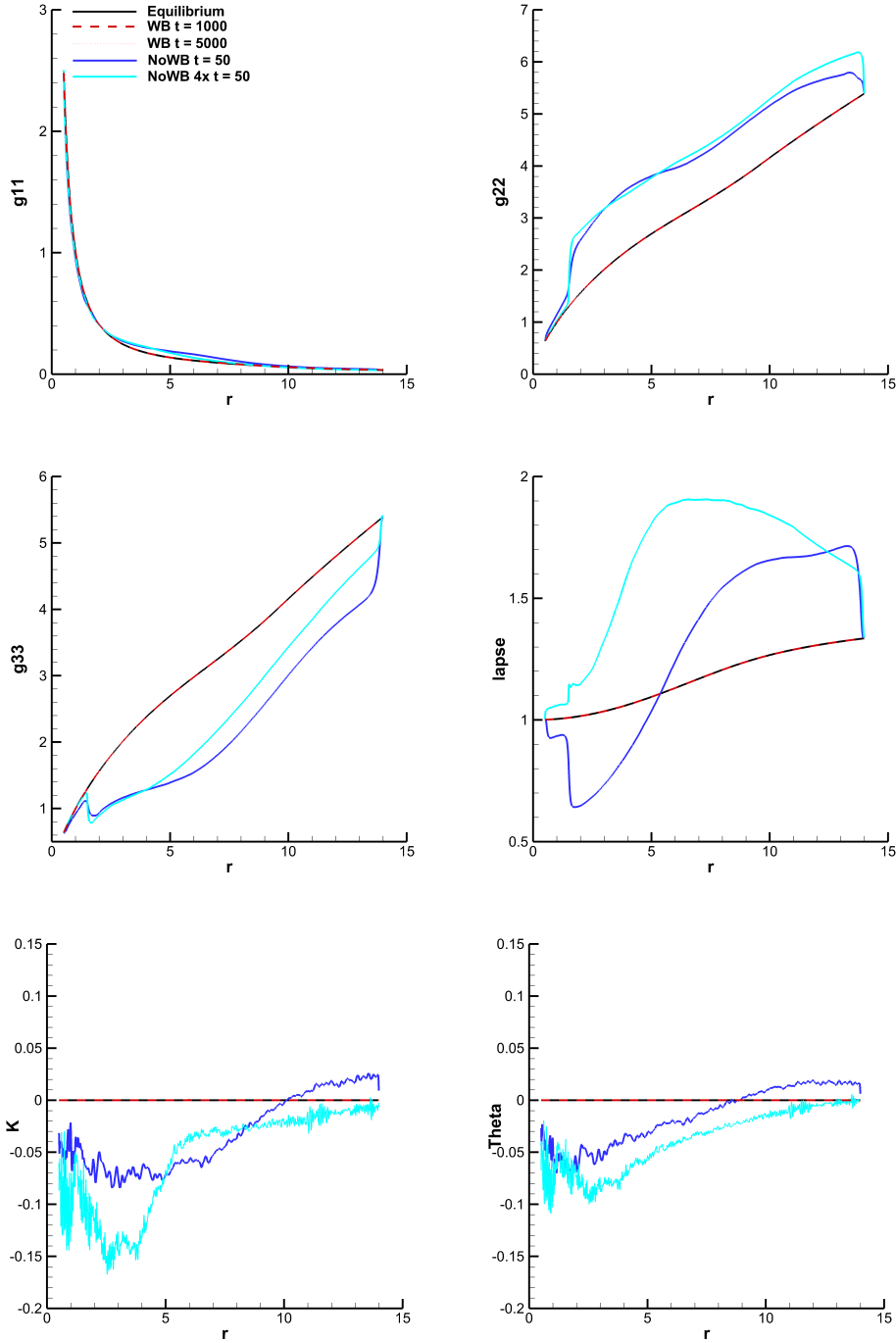


FIG. 7. TOV star simulation with the CCZ4+GRHD fully coupled model corresponding to an initial perturbation over the metric variable K . We show: *i*) the expected equilibrium profile to be recovered once the perturbation has exited the domain (black line), *ii*) the numerical results obtained with the new WB scheme at very long times ($t = 1000$ in red and $t = 5000$ in pink) and *iii*) the completely corrupted results obtained with the not WB scheme already after a very short computational time $t = 50$ (blue) even on a four time finer mesh (cyan). Plotted variables: the diagonal components of the metric γ_{11} , γ_{22} , γ_{33} , the lapse function λ , the extrinsic curvature K and the cleaning variable θ .

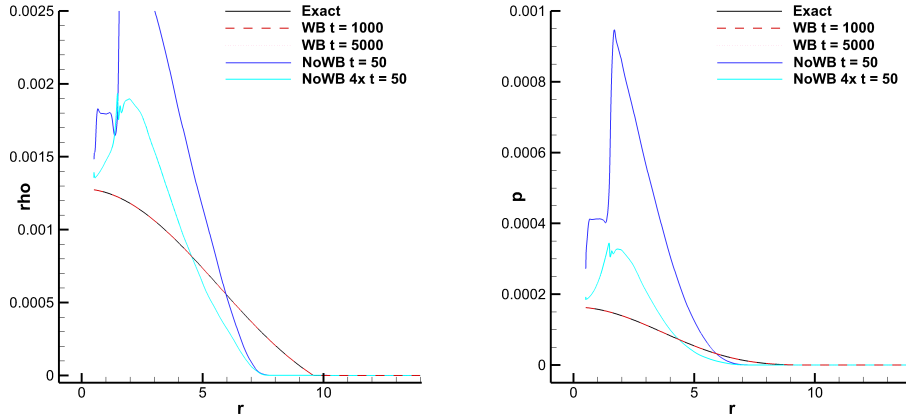


FIG. 8. TOV star simulation with the CCZ_4+GRHD fully coupled model corresponding to an initial perturbation over the metric variable K . With the same color map of the previous Figure we show here the effects of a perturbation over the metric variable K on matter variables as density ρ (left) and pressure p (right).

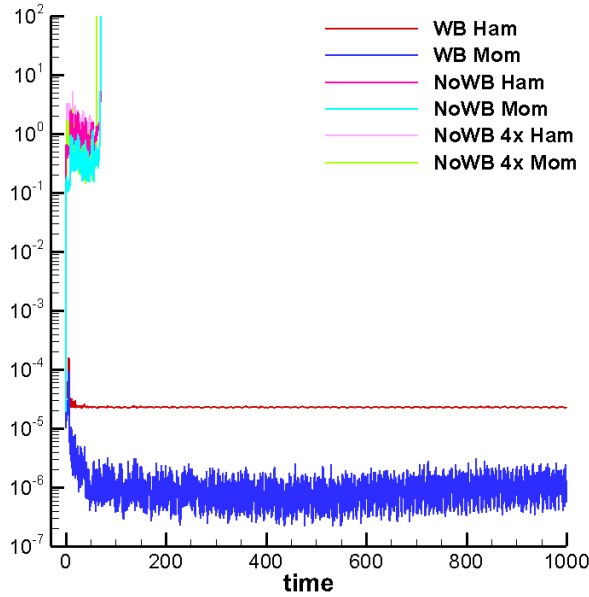


FIG. 9. Hamiltonian (Ham) and momentum (Mom) constraints for the TOV star simulation with the fully coupled model over the time $t \in [0, 1000]$. Note again the initial pick, the more closer to machine precision values obtained with the WB schemes already at the beginning of the simulation and in particular the fact that with the not WB code the constraints, as the entire simulation, completely blows up after a brief time while the WB code always provided trustable numerical results as evident from the perfect constraints preservation.

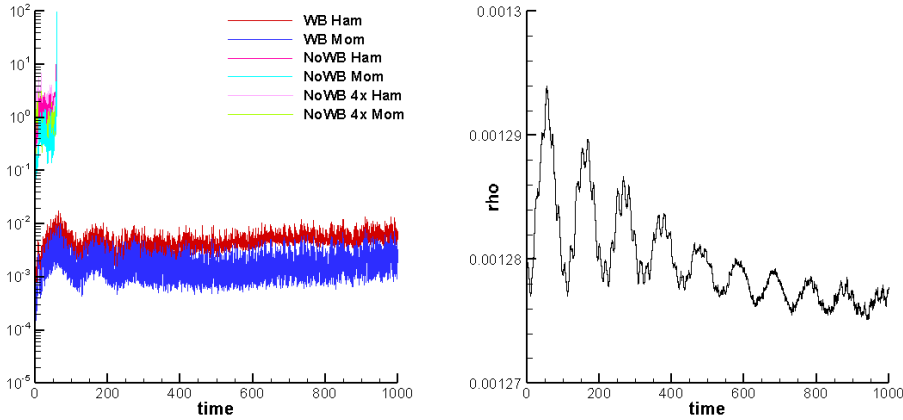


FIG. 10. TOV star simulation with the $CCZ4+GRHD$ fully coupled model corresponding to an initial perturbation over the pressure profile p . Left: we show the values of the Hamiltonian and momentum constraints which are close to machine precision and constantly maintained for long computational times with the WB code, while they rapidly blow up with the not WB code. Right: we plot the numerical results obtained with the new WB scheme for the density of the star at an inner point with $r = 0.5$ which oscillates due to the initial pressure perturbations.

536 soon with the not WB scheme.

537 **Perturbation of the matter variable \mathbf{p} .** Next, we study the effect of a small
 538 pressure perturbation as the one given in (4.5) where, for what concerns the sponge
 539 layer, we activate it only for the right boundary, and we choose $s_{\mathcal{L}} = 0$, $s_{\mathcal{R}} = 3$ and
 540 $\varepsilon_R = 10^{-4}$. Once again the constraints are more precise and better preserved with
 541 the WB scheme, see Figure 10.

542 For what concerns the mass oscillation at an internal point with $r = 0.5$ in
 543 Figure 10 we report only the results obtained with the new WB scheme, since the not
 544 WB method, even on finer meshes, explodes after a very short time. Comparing the
 545 amplitude of this oscillation with those obtained on a fixed space-time in Figure 4 one
 546 can appreciate the different dynamic behavior obtained with a fully coupled model,
 547 where the interaction between metric and mass are taken into account, compared to
 548 the simpler GRMHD model in Cowling approximation with fixed space-time.

549

550 4.4. Numerical convergence studies for our well balanced algorithm.

551 For the sake of completeness, in this last section we check the convergence rate of
 552 our new well balanced scheme by computing the experimental errors committed when
 553 solving the Michel accretion disk test case, which is an equilibrium solution of the
 554 GRMHD system known analytically (see Section 4.1), while preserving completely
 555 different equilibrium profiles, namely a i) fluid at rest immersed in a flat space-time
 556 and ii) the TOV neutron star of the previous Section 4.3. The choice of using an initial
 557 condition that completely differs from the equilibrium profiles to be preserved allows
 558 to show the second order of convergence of our well balanced method; the scheme
 559 would be instead *exact* when choosing to preserve an equilibrium that is equal to
 560 the initial condition of the test problem. The obtained numerical results are shown in
 561 Table 2; we would like to emphasize that the order of convergence is correctly retained
 562 even for long computational times.

TABLE 2

L_2 norm of the experimental errors and order of accuracy at times $t = 1, 10, 100$ and 1000 for the density variable ρ of the Michel accretion disk test case simulated with our well balanced scheme set to preserve *i*) a fluid at rest over a flat space-time (top) and *ii*) a TOV Neutron star (bottom).

Flat ST Δx	$t = 1$		$t = 10$		$t = 100$		$t = 1000$	
	L_2	$\mathcal{O}(L_2)$	L_2	$\mathcal{O}(L_2)$	L_2	$\mathcal{O}(L_2)$	L_2	$\mathcal{O}(L_2)$
9.0E-03	3.1E-06	-	4.9E-05	-	5.9E-04	-	5.0E-03	-
6.0E-03	1.4E-06	1.99	2.2E-05	1.93	2.7E-04	1.88	2.4E-03	1.79
4.5E-03	8.0E-07	1.95	1.3E-05	1.95	1.6E-04	1.91	1.4E-03	1.82
3.6E-03	5.1E-07	1.98	8.3E-06	1.96	1.0E-04	1.92	9.5E-04	1.84
3.0E-03	3.6E-07	1.97	5.8E-06	1.96	7.3E-05	1.93	6.8E-04	1.86
TOV star Δx	$t = 1$		$t = 10$		$t = 100$		$t = 1000$	
	L_2	$\mathcal{O}(L_2)$	L_2	$\mathcal{O}(L_2)$	L_2	$\mathcal{O}(L_2)$	L_2	$\mathcal{O}(L_2)$
9.0E-03	2.7E-06	-	5.6E-05	-	7.2E-04	-	6.3E-03	-
6.0E-03	1.2E-06	1.99	2.6E-05	1.92	3.3E-04	1.89	3.0E-03	1.81
4.5E-03	6.9E-07	1.94	1.5E-05	1.94	1.9E-04	1.91	1.8E-03	1.84
3.6E-03	4.4E-07	1.98	9.6E-06	1.95	1.3E-04	1.92	1.2E-03	1.86
3.0E-03	3.1E-07	1.97	6.7E-06	1.96	8.8E-05	1.93	8.4E-04	1.87

563 **5. Conclusions.** With the numerical results presented here we have clearly
564 shown the advantages that can be obtained in numerical general relativity through the
565 use of a simple but very efficient well balancing technique. Indeed, simulations that
566 blow up with a standard second order scheme can now be carried out in a stable man-
567 ner even for very long simulation times and with accurate results, as demonstrated
568 for example by the monitoring of the ADM constraints and the simulations carried
569 out with the fully coupled FO-CCZ4 + GRMHD model. Moreover, we would like
570 to underline that this preliminary work in 1D at second order of accuracy has been
571 essential to understand model related difficulties how the setting of the cleaning and
572 damping parameters in the FO-CCZ4 model and the boundary conditions.

573 Future work will concern the insertion of the presented WB techniques in already
574 existing higher order discontinuous Galerkin schemes for modeling the GRMHD and
575 the FO-CCZ4 systems in two or three space dimensions, as those presented in [55, 63].
576 In this context we will follow also the numerical approach presented in [102, 101].
577 Moreover, we would like to investigate the joint effect of WB and the novel GLM
578 curl cleaning techniques introduced in [54, 43, 35]. Indeed, several systems with curl
579 involutions have recently been investigated and attention has been devoted to the
580 crucial role of curl involutions themselves [53] on the stability of numerical computa-
581 tions. With the increased level of robustness and accuracy that can be obtained at
582 the aid of the new well balanced schemes introduced in this paper, in combination
583 with high order DG schemes and novel curl cleaning techniques, it should therefore
584 become possible to study also the generation and propagation of *gravitational waves*
585 in the future.

586 Furthermore, motivated by the results obtained in [62] for the study of Kep-
587 lerian disks modeled with the Euler equations with gravity and simulated with a
588 well balanced *Lagrangian* scheme, we would like to apply a similar approach also
589 for the study of general relativistic phenomena; in particular, we plan to incorpo-
590 rate our new well balanced techniques for GRMHD and FO-CCZ4 in modern direct

591 Arbitrary-Lagrangian Eulerian algorithms with topology changes, as those forwarded
592 in [90, 64, 60, 59, 44].

593 **Acknowledgments.** E. G gratefully acknowledges the support received from the
594 European Union’s Horizon 2020 Research and Innovation Programme under the Marie
595 Skłodowska-Curie Individual Fellowship *SuPerMan*, grant agreement No. 101025563.
596 E. G. has been also supported by a national mobility grant for young researchers
597 in Italy funded by GNCS-INdAM, and she received funding from the University of
598 Trento via the Strategic Initiative *Starting Grant Giovani Ricercatori 2019*.

599 Moreover, the research presented in this paper has been partially funded by
600 the European Union’s Horizon 2020 Research and Innovation Programme under the
601 project *ExaHyPE*, grant No. 671698 (call FETHPC-1-2014).

602 M. D. also acknowledges the financial support received from the Italian Ministry
603 of Education, University and Research (MIUR) in the frame of the Departments of Ex-
604 cellence Initiative 2018–2022 attributed to DICAM of the University of Trento (grant
605 L. 232/2016) and in the frame of the PRIN 2017 project *Innovative numerical methods*
606 *for evolutionary partial differential equations and applications*. Furthermore, M. D.
607 has also received funding from the University of Trento via the Strategic Initiative
608 *Modeling and Simulation*.

609 The research of M.J. Castro was partially supported by the Spanish Govern-
610 ment (SG), the European Regional Development Fund (ERDF), the Regional Govern-
611 ment of Andalusia (RGA), and the University of Málaga(UMA) through the projects
612 of references RTI2018-096064-B-C21 (SG-ERDF), UMA18-Federja-161 (RGA-ERDF-
613 UMA), and P18-RT-3163 (RGA-ERDF).

614 E.G. is member of the CARDAMOM team at Inria BSO (France), M.D. is member
615 of the INdAM-GNCS group (Italy), and M. J. Castro is member of the EDANYA
616 group (Spain).

617

REFERENCES

- 618 [1] M. ALCUBIERRE, *Introduction to 3+1 numerical relativity*, vol. 140, Oxford University Press,
619 2008.
- 620 [2] D. ALIC, C. BONA, AND C. BONA-CASAS, *Towards a gauge-polyvalent numerical relativity*
621 *code*, Physical Review D, 79 (2009), p. 044026.
- 622 [3] D. ALIC, C. BONA-CASAS, C. BONA, L. REZZOLLA, AND C. PALENZUELA, *Conformal and co-*
623 *variant formulation of the Z_4 system with constraint-violation damping*, Physical Review
624 D, 85 (2012), p. 064040.
- 625 [4] D. ALIC, W. KASTAUN, AND L. REZZOLLA, *Constraint damping of the conformal and covariant*
626 *formulation of the Z_4 system in simulations of binary neutron stars*, Physical Review D,
627 88 (2013), p. 064049.
- 628 [5] M.-Á. ALOY AND I. CORDERO-CARRIÓN, *Minimally implicit Runge-Kutta methods for Resis-*
629 *tive Relativistic MHD*, in Journal of Physics: Conference Series, vol. 719, IOP Publishing,
630 2016, p. 012015.
- 631 [6] M. A. ALOY, J. M. IBÁÑEZ, J. M. MARTÍ, AND E. MÜLLER, *GENESIS: A high-resolution code*
632 *for three-dimensional relativistic hydrodynamics*, The Astrophysical Journal Supplement
633 Series, 122 (1999), p. 151.
- 634 [7] M. ANDERSON, E. W. HIRSCHMANN, L. LEHNER, S. L. LIEBLING, P. M. MOTL, D. NEILSEN,
635 C. PALENZUELA, AND J. E. TOHLIN, *Magnetized neutron-star mergers and gravitational-*
636 *wave signals*, Physical Review Letters, 100 (2008), p. 191101.
- 637 [8] A. ANILE, *Relativistic Fluids and Magneto-fluids ed AM Anile (Cambridge, UK)*, 1990.
- 638 [9] A. ANILE, J. MILLER, AND S. MOTTA, *Formation and damping of relativistic strong shocks*,
639 The Physics of Fluids, 26 (1983), pp. 1450–1460.
- 640 [10] P. ANNINOS, P. C. FRAGILE, AND J. D. SALMONSON, *Cosmos++: relativistic magnetohydro-*
641 *dynamics on unstructured grids with local adaptive refinement*, The Astrophysical Journal,
642 635 (2005), p. 723.

- 643 [11] L. ANTÓN, O. ZANOTTI, J. A. MIRALLES, J. M. MARTÍ, J. M. IBÁÑEZ, J. A. FONT, AND J. A.
 644 PONS, *Numerical 3+1 general relativistic magnetohydrodynamics: a local characteristic*
 645 *approach*, The Astrophysical Journal, 637 (2006), p. 296.
- 646 [12] R. ARNOWITT, S. DESER, AND C. W. MISNER, *The dynamics of general relativity, Gravitation:*
 647 *An introduction to current research*, Chap. 7 (1962), pp. 227–265.
- 648 [13] R. ARNOWITT, S. DESER, AND C. W. MISNER, *Republication of: The dynamics of general*
 649 *relativity*, General Relativity and Gravitation, 40 (2008), pp. 1997–2027.
- 650 [14] L. ARPAIA AND M. RICCHIUTO, *Well balanced residual distribution for the ale spherical shal-*
 651 *low water equations on moving adaptive meshes*, Journal of Computational Physics, 405
 652 (2020), p. 109173.
- 653 [15] E. AUDUSSE, F. BOUCHUT, M.-O. BRISTEAU, R. KLEIN, AND B. T. PERTHAME, *A fast and*
 654 *stable well-balanced scheme with hydrostatic reconstruction for shallow water flows*, SIAM
 655 Journal on Scientific Computing, 25 (2004), pp. 2050–2065.
- 656 [16] L. BAIOTTI, I. HAWKE, P. J. MONTERO, F. LÖFFLER, L. REZZOLLA, N. STERGIOLAS, J. A.
 657 FONT, AND E. SEIDEL, *Three-dimensional relativistic simulations of rotating neutron-star*
 658 *collapse to a Kerr black hole*, Physical Review D, 71 (2005), p. 024035.
- 659 [17] F. BANYULS, J. A. FONT, J. M. IBÁÑEZ, J. M. MARTÍ, AND J. A. MIRALLES, *Numerical {3+1}*
 660 *general relativistic hydrodynamics: A local characteristic approach*, The Astrophysical
 661 Journal, 476 (1997), p. 221.
- 662 [18] C. BASSI, L. BONAVENTURA, S. BUSTO, AND M. DUMBSER, *A hyperbolic reformulation of*
 663 *the Serre-Green-Naghdi model for general bottom topographies*, Computers & Fluids, 212
 664 (2020), p. 104716.
- 665 [19] T. W. BAUMGARTE AND S. L. SHAPIRO, *Numerical integration of Einstein’s field equations*,
 666 Physical Review D, 59 (1998), p. 024007.
- 667 [20] T. W. BAUMGARTE AND S. L. SHAPIRO, *Numerical relativity: solving Einstein’s equations on*
 668 *the computer*, Cambridge University Press, 2010.
- 669 [21] J. P. BERBERICH, P. CHANDRASHEKAR, AND C. KLINGENBERG, *High order well-balanced finite*
 670 *volume methods for multi-dimensional systems of hyperbolic balance laws*, Computers &
 671 Fluids, (2021), p. 104858.
- 672 [22] A. BERMÚDEZ, X. LÓPEZ, AND M. E. VÁZQUEZ-CENDÓN, *Numerical solution of non-isothermal*
 673 *non-adiabatic flow of real gases in pipelines*, Journal of Computational Physics, 323
 674 (2016), pp. 126–148.
- 675 [23] A. BERMUDEZ AND M. E. VAZQUEZ, *Upwind methods for hyperbolic conservation laws with*
 676 *source terms*, Computers & Fluids, 23 (1994), pp. 1049–1071.
- 677 [24] S. BERNUZZI AND D. HILDITCH, *Constraint violation in free evolution schemes: Comparing the*
 678 *BSSNOK formulation with a conformal decomposition of the Z4 formulation*, Physical
 679 Review D, 81 (2010), p. 084003.
- 680 [25] C. BONA, T. LEDVINKA, C. PALENZUELA, AND M. ZÁČEK, *General-covariant evolution for-*
 681 *malism for numerical relativity*, Phys. Rev. D, 67 (2003), p. 104005.
- 682 [26] C. BONA, T. LEDVINKA, C. PALENZUELA, AND M. ZÁČEK, *Symmetry-breaking mechanism for*
 683 *the Z4 general-covariant evolution system*, Phys. Rev. D, 69 (2004), p. 64036.
- 684 [27] C. BONA, J. MASSO, E. SEIDEL, AND J. STELA, *New formalism for numerical relativity*,
 685 Physical Review Letters, 75 (1995), p. 600.
- 686 [28] S. BONAZZOLA, E. GOURGOULHON, P. GRANDCLEMENT, AND J. NOVAK, *Constrained scheme*
 687 *for the einstein equations based on the dirac gauge and spherical coordinates*, Physical
 688 Review D, 70 (2004), p. 104007.
- 689 [29] N. BOTTA, R. KLEIN, S. LANGENBERG, AND S. LÜTZENKIRCHEN, *Well balanced finite vol-*
 690 *ume methods for nearly hydrostatic flows*, Journal of Computational Physics, 196 (2004),
 691 pp. 539–565.
- 692 [30] F. BOUCHUT, *Nonlinear stability of finite Volume Methods for hyperbolic conservation laws:*
 693 *And Well-Balanced schemes for sources*, Springer Science & Business Media, 2004.
- 694 [31] N. BUCCIANINI AND L. DEL ZANNA, *General relativistic magnetohydrodynamics in axisym-*
 695 *metric dynamical spacetimes: the X-ECHO code*, Astronomy & Astrophysics, 528 (2011),
 696 p. A101.
- 697 [32] N. BUCCIANINI AND L. DEL ZANNA, *A fully covariant mean-field dynamo closure for nu-*
 698 *merical 3+1 resistive GRMHD*, Monthly Notices of the Royal Astronomical Society, 428
 699 (2013), pp. 71–85.
- 700 [33] M. BUGLI, L. DEL ZANNA, AND N. BUCCIANINI, *Dynamo action in thick discs around Kerr*
 701 *black holes: high-order resistive GRMHD simulations*, Monthly Notices of the Royal
 702 Astronomical Society: Letters, 440 (2014), pp. L41–L45.
- 703 [34] M. BUGNER, *Discontinuous Galerkin methods for general relativistic hydrodynamics*, PhD
 704 thesis, Friedrich-Schiller-Universität Jena, 2018.

- 705 [35] S. BUSTO, M. DUMBSER, C. ESCALANTE, S. GAVRILYUK, AND N. FAVRIE, *On high order ADER*
706 *discontinuous Galerkin schemes for first order hyperbolic reformulations of nonlinear*
707 *dispersive systems*, Journal of Scientific Computing, 87 (2021), p. 48.
- 708 [36] S. CARROLL, *Spacetime and geometry. An introduction to general relativity*, 2003.
- 709 [37] M. CASTRO, J. GALLARDO, AND C. PARÉS, *High order finite volume schemes based on recon-*
710 *struction of states for solving hyperbolic systems with nonconservative products. Applica-*
711 *tions to shallow-water systems*, Mathematics of computation, 75 (2006), pp. 1103–1134.
- 712 [38] M. CASTRO, J. M. GALLARDO, J. A. LÓPEZ-GARCÍA, AND C. PARÉS, *Well-balanced high order*
713 *extensions of Godunov’s method for semilinear balance laws*, SIAM Journal on Numerical
714 Analysis, 46 (2008), pp. 1012–1039.
- 715 [39] M. J. CASTRO, T. M. DE LUNA, AND C. PARÉS, *Chapter 6 - Well-balanced schemes and path-*
716 *conservative numerical methods*, in Handbook of Numerical Analysis, vol. 18, Elsevier,
717 2017, pp. 131–175.
- 718 [40] M. J. CASTRO AND C. PARÉS, *Well-balanced high-order finite volume methods for systems of*
719 *balance laws*, Journal of Scientific Computing, 82 (2020), pp. 1–48.
- 720 [41] P. CHANDRASHEKAR AND C. KLINGENBERG, *A second order well-balanced finite volume scheme*
721 *for Euler equations with gravity*, SIAM Journal on Scientific Computing, 37 (2015),
722 pp. B382–B402.
- 723 [42] A. Y. CHERNYSHENKO, M. A. OLSHANSKII, AND Y. V. VASSILEVSKI, *A hybrid finite volume–*
724 *finite element method for bulk–surface coupled problems*, Journal of Computational
725 Physics, 352 (2018), pp. 516–533.
- 726 [43] S. CHIOCCETTI, I. PESHKOV, S. GAVRILYUK, AND M. DUMBSER, *High order ADER schemes*
727 *and GLM curl cleaning for a first order hyperbolic formulation of compressible flow with*
728 *surface tension*, Journal of Computational Physics, 426 (2021), p. 109898.
- 729 [44] L. CIRROTTOLA, M. RICCHIUTO, A. FROEHLI, B. RE, A. GUARDONE, AND G. QUARANTA,
730 *Adaptive deformation of 3d unstructured meshes with curved body fitted boundaries with*
731 *application to unsteady compressible flows*, Journal of Computational Physics, 433 (2021),
732 p. 110177.
- 733 [45] I. CORDERO-CARRIÓN, P. CERDÁ-DURÁN, H. DIMMELMEIER, J. L. JARAMILLO, J. NOVAK, AND
734 E. GOURGOLHON, *Improved constrained scheme for the einstein equations: An approach*
735 *to the uniqueness issue*, Physical Review D, 79 (2009), p. 024017.
- 736 [46] I. CORDERO-CARRIÓN, J. M. IBANEZ, E. GOURGOLHON, J. L. JARAMILLO, AND J. NOVAK,
737 *Mathematical issues in a fully constrained formulation of the einstein equations*, Physical
738 Review D, 77 (2008), p. 084007.
- 739 [47] G. DAL MASO, P. G. LEFLOCH, AND F. MURAT, *Definition and weak stability of nonconser-*
740 *vative products*, Journal de mathématiques pures et appliquées, 74 (1995), pp. 483–548.
- 741 [48] L. DEL ZANNA AND N. BUCCIANTINI, *An efficient shock-capturing central-type scheme for*
742 *multidimensional relativistic flows-I. Hydrodynamics*, Astronomy & Astrophysics, 390
743 (2002), pp. 1177–1186.
- 744 [49] L. DEL ZANNA, O. ZANOTTI, N. BUCCIANTINI, AND P. LONDRILLO, *ECHO: a Eulerian con-*
745 *servative high-order scheme for general relativistic magnetohydrodynamics and magne-*
746 *todynamics*, Astronomy & Astrophysics, 473 (2007), pp. 11–30.
- 747 [50] V. DESVEAUX, M. ZENK, C. BERTHON, AND C. KLINGENBERG, *A well-balanced scheme to cap-*
748 *ture non-explicit steady states in the Euler equations with gravity*, International Journal
749 for Numerical Methods in Fluids, 81 (2016), pp. 104–127.
- 750 [51] K. DIONYSOPOULOU, D. ALIC, C. PALENZUELA, L. REZZOLLA, AND B. GIACOMAZZO, *General-*
751 *relativistic resistive magnetohydrodynamics in three dimensions: Formulation and tests*,
752 Physical Review D, 88 (2013), p. 044020.
- 753 [52] M. D. DUEZ, Y. T. LIU, S. L. SHAPIRO, AND B. C. STEPHENS, *Relativistic magnetohydrody-*
754 *namics in dynamical spacetimes: Numerical methods and tests*, Physical Review D, 72
755 (2005), p. 024028.
- 756 [53] M. DUMBSER, S. CHIOCCETTI, AND I. PESHKOV, *On numerical methods for hyperbolic pde*
757 *with curl involutions*, Continuum Mechanics, Applied Mathematics and Scientific Com-
758 puting: Godunov’s Legacy, Springer, (2020), pp. 125–134.
- 759 [54] M. DUMBSER, F. FAMBRI, E. GABURRO, AND A. REINARZ, *On GLM curl cleaning for a*
760 *first order reduction of the CCZ4 formulation of the Einstein field equations*, Journal of
761 Computational Physics, 404 (2020), p. 109088.
- 762 [55] M. DUMBSER, F. GUERCILENA, S. KÖPPEL, L. REZZOLLA, AND O. ZANOTTI, *Conformal and*
763 *covariant Z4 formulation of the Einstein equations: Strongly hyperbolic first-order reduc-*
764 *tion and solution with discontinuous Galerkin schemes*, Physical Review D, 97 (2018),
765 p. 084053.
- 766 [56] M. DUMBSER AND O. ZANOTTI, *Very high order PNPM schemes on unstructured meshes for*

- 767 *the resistive relativistic MHD equations*, Journal of Computational Physics, 228 (2009),
768 pp. 6991–7006.
- 769 [57] F. FAMBRI, M. DUMBSER, S. KÖPPEL, L. REZZOLLA, AND O. ZANOTTI, *ADER discontinuous*
770 *Galerkin schemes for general-relativistic ideal magnetohydrodynamics*, Monthly Notices
771 of the Royal Astronomical Society, 477 (2018), pp. 4543–4564.
- 772 [58] J. A. FONT, *Numerical hydrodynamics and magnetohydrodynamics in general relativity*, Liv-
773 ing Reviews in Relativity, 11 (2008), pp. 1–131.
- 774 [59] E. GABURRO, *A Unified Framework for the Solution of Hyperbolic PDE Systems Using High*
775 *Order Direct Arbitrary-Lagrangian–Eulerian Schemes on Moving Unstructured Meshes*
776 *with Topology Change*, Archives of Computational Methods in Engineering, (2020).
- 777 [60] E. GABURRO, W. BOSCHERI, S. CHIOCCETTI, C. KLINGENBERG, V. SPRINGEL, AND M. DUMB-
778 SER, *High order direct Arbitrary-Lagrangian-Eulerian schemes on moving Voronoi meshes*
779 *with topology changes*, Journal of Computational Physics, 407 (2020), p. 109167.
- 780 [61] E. GABURRO, M. J. CASTRO, AND M. DUMBSER, *A well balanced diffuse interface method for*
781 *complex nonhydrostatic free surface flows*, Computers & Fluids, 175 (2018), pp. 180–198.
- 782 [62] E. GABURRO, M. J. CASTRO, AND M. DUMBSER, *Well-balanced Arbitrary-Lagrangian-Eulerian*
783 *finite volume schemes on moving nonconforming meshes for the Euler equations of gas*
784 *dynamics with gravity*, Monthly Notices of the Royal Astronomical Society, 477 (2018),
785 pp. 2251–2275.
- 786 [63] E. GABURRO AND M. DUMBSER, *A Posteriori Subcell Finite Volume Limiter for General*
787 *PNPM Schemes: Applications from Gasdynamics to Relativistic Magnetohydrodynamics*,
788 Journal of Scientific Computing, 86 (2021), pp. 1–41.
- 789 [64] E. GABURRO, M. DUMBSER, AND M. J. CASTRO, *Direct Arbitrary-Lagrangian-Eulerian finite*
790 *volume schemes on moving nonconforming unstructured meshes*, Computers & Fluids,
791 159 (2017), pp. 254–275.
- 792 [65] B. GIACOMAZZO AND L. REZZOLLA, *WhiskyMHD: a new numerical code for general relativistic*
793 *magnetohydrodynamics*, Classical and Quantum Gravity, 24 (2007), p. S235.
- 794 [66] L. GOSSE, *A well-balanced scheme using non-conservative products designed for hyperbolic*
795 *systems of conservation laws with source terms*, Mathematical Models and Methods in
796 Applied Sciences, 11 (2001), pp. 339–365.
- 797 [67] L. GROSHEINTZ-LAVAL AND R. KÄPPEL, *High-order well-balanced finite volume schemes for*
798 *the Euler equations with gravitation*, Journal of Computational Physics, 378 (2019),
799 pp. 324–343.
- 800 [68] C. GUNDLACH AND J. M. MARTIN-GARCIA, *Hyperbolicity of second order in space systems of*
801 *evolution equations*, Classical and Quantum Gravity, 23 (2006), p. S387.
- 802 [69] R. KÄPPEL AND S. MISHRA, *Well-balanced schemes for the Euler equations with gravitation*,
803 Journal of Computational Physics, 259 (2014), pp. 199–219.
- 804 [70] R. KÄPPEL AND S. MISHRA, *A well-balanced finite volume scheme for the euler equations*
805 *with gravitation—the exact preservation of hydrostatic equilibrium with arbitrary entropy*
806 *stratification*, Astronomy & Astrophysics, 587 (2016), p. A94.
- 807 [71] K. KIUCHI, Y. SEKIGUCHI, M. SHIBATA, AND K. TANIGUCHI, *Long-term general relativistic*
808 *simulation of binary neutron stars collapsing to a black hole*, Physical Review D, 80
809 (2009), p. 064037.
- 810 [72] C. KLINGENBERG, G. PUPPO, AND M. SEMPLICE, *Arbitrary order finite volume well-balanced*
811 *schemes for the Euler equations with gravity*, SIAM Journal on Scientific Computing, 41
812 (2019), pp. A695–A721.
- 813 [73] S. KOMISSAROV, *General relativistic magnetohydrodynamic simulations of monopole magne-*
814 *tospheres of black holes*, Monthly Notices of the Royal Astronomical Society, 350 (2004),
815 pp. 1431–1436.
- 816 [74] R. J. LEVEQUE, *Balancing source terms and flux gradients in high-resolution Godunov meth-*
817 *ods: the quasi-steady wave-propagation algorithm*, Journal of computational physics, 146
818 (1998), pp. 346–365.
- 819 [75] J. M. MARTÍ AND E. MÜLLER, *Grid-based methods in relativistic hydrodynamics and magne-*
820 *tohydrodynamics*, Living reviews in computational astrophysics, 1 (2015), pp. 1–182.
- 821 [76] F. C. MICHEL, *Accretion of matter by condensed objects*, Astrophysics and Space Science, 15
822 (1972), pp. 153–160.
- 823 [77] T. NAKAMURA, K. OOHARA, AND Y. KOJIMA, *General relativistic collapse to black holes and*
824 *gravitational waves from black holes*, Progress of Theoretical Physics Supplement, 90
825 (1987), pp. 1–218.
- 826 [78] J. R. OPPENHEIMER AND G. M. VOLKOFF, *On massive neutron cores*, Physical Review, 55
827 (1939), p. 374.
- 828 [79] C. PALENZUELA, L. LEHNER, O. REULA, AND L. REZZOLLA, *Beyond ideal MHD: towards*

- 829 *a more realistic modelling of relativistic astrophysical plasmas*, Monthly Notices of the
 830 Royal Astronomical Society, 394 (2009), pp. 1727–1740.
- 831 [80] C. PARÉS, *Numerical methods for nonconservative hyperbolic systems: a theoretical frame-*
 832 *work.*, SIAM Journal on Numerical Analysis, 44 (2006), pp. 300–321.
- 833 [81] B. PERTHAME AND C. SIMEONI, *A kinetic scheme for the Saint-Venant system with a source*
 834 *term*, Calcolo, 38 (2001), pp. 201–231.
- 835 [82] O. PORTH, H. OLIVARES, Y. MIZUNO, Z. YOUNSI, L. REZZOLLA, M. MOSCIBRODZKA, H. FAL-
 836 *CKE*, AND M. KRAMER, *The black hole accretion code*, Computational Astrophysics and
 837 *Cosmology*, 4 (2017), pp. 1–42.
- 838 [83] D. RADICE AND L. REZZOLLA, *THC: a new high-order finite-difference high-resolution shock-*
 839 *capturing code for special-relativistic hydrodynamics*, Astronomy & Astrophysics, 547
 840 (2012), p. A26.
- 841 [84] D. RADICE, L. REZZOLLA, AND F. GALEAZZI, *Beyond second-order convergence in simula-*
 842 *tions of binary neutron stars in full general relativity*, Monthly Notices of the Royal
 843 *Astronomical Society: Letters*, 437 (2013), pp. L46–L50.
- 844 [85] T. C. REBOLLO, A. D. DELGADO, AND E. D. F. NIETO, *A family of stable numerical solvers for*
 845 *the shallow water equations with source terms*, Computer methods in applied mechanics
 846 *and engineering*, 192 (2003), pp. 203–225.
- 847 [86] L. REZZOLLA AND O. ZANOTTI, *Relativistic hydrodynamics*, Oxford University Press, 2013.
- 848 [87] G. RUSSO AND A. ANILE, *Stability properties of relativistic shock waves: basic results*, The
 849 *Physics of fluids*, 30 (1987), pp. 2406–2413.
- 850 [88] K. SCHAAL, A. BAUER, P. CHANDRASHEKAR, R. PAKMOR, C. KLINGENBERG, AND V. SPRINGEL,
 851 *Astrophysical hydrodynamics with a high-order discontinuous Galerkin scheme and adap-*
 852 *tive mesh refinement*, Monthly Notices of the Royal Astronomical Society, 453 (2015),
 853 pp. 4278–4300.
- 854 [89] M. SHIBATA AND T. NAKAMURA, *Evolution of three-dimensional gravitational waves: Har-*
 855 *monic slicing case*, Physical Review D, 52 (1995), p. 5428.
- 856 [90] V. SPRINGEL, *E pur si muove: Galilean-invariant cosmological hydrodynamical simulations on*
 857 *a moving mesh*, Monthly Notices of the Royal Astronomical Society, 401 (2010), pp. 791–
 858 851.
- 859 [91] R. TAKAHASHI AND M. UMEMURA, *General relativistic radiative transfer code in rotating*
 860 *black hole space-time: ARTIST*, Monthly Notices of the Royal Astronomical Society, 464
 861 (2016), pp. 4567–4585.
- 862 [92] H. TANG, T. TANG, AND K. XU, *A gas-kinetic scheme for shallow-water equations with source*
 863 *terms*, Zeitschrift für angewandte Mathematik und Physik ZAMP, 55 (2004), pp. 365–382.
- 864 [93] A. THOMANN, M. ZENK, AND C. KLINGENBERG, *A second-order positivity-preserving well-*
 865 *balanced finite volume scheme for Euler equations with gravity for arbitrary hydrostatic*
 866 *equilibria*, International Journal for Numerical Methods in Fluids, 89 (2019), pp. 465–482.
- 867 [94] R. C. TOLMAN, *Static solutions of Einstein’s field equations for spheres of fluid*, Physical
 868 *Review*, 55 (1939), p. 364.
- 869 [95] E. F. TORO, *Riemann Solvers and Numerical Methods for Fluid Dynamics*, Springer, sec-
 870 *ond ed.*, 1999.
- 871 [96] B. VAN LEER, *Towards the ultimate conservative difference scheme. II. Monotonicity and*
 872 *conservation combined in a second-order scheme*, Journal of computational physics, 14
 873 (1974), pp. 361–370.
- 874 [97] B. VAN LEER, *Towards the ultimate conservative difference scheme. V. A second-order sequel*
 875 *to Godunov’s method*, Journal of computational Physics, 32 (1979), pp. 101–136.
- 876 [98] R. M. WALD, *General relativity(Book)*, Chicago, University of Chicago Press, 1984, 504 p,
 877 (1984).
- 878 [99] C. J. WHITE, J. M. STONE, AND C. F. GAMMIE, *An extension of the Athena++ code frame-*
 879 *work for GRMHD based on advanced Riemann solvers and staggered-mesh constrained*
 880 *transport*, The Astrophysical Journal Supplement Series, 225 (2016), p. 22.
- 881 [100] J. R. WILSON, *Some magnetic effects in stellar collapse and accretion*, tech. report, California
 882 *Univ., Livermore (USA)*. Lawrence Livermore Lab., 1975.
- 883 [101] Y. XING, *Exactly well-balanced discontinuous Galerkin methods for the shallow water equa-*
 884 *tions with moving water equilibrium*, Journal of Computational Physics, 257 (2014),
 885 pp. 536–553.
- 886 [102] Y. XING AND C.-W. SHU, *High order well-balanced finite volume WENO schemes and discon-*
 887 *tinuous Galerkin methods for a class of hyperbolic systems with source terms*, Journal of
 888 *Computational Physics*, 214 (2006), pp. 567–598.